



<p>The University of Edinburgh</p> 	<p>ATSR Reprocessing for Climate Lake Surface Water Temperature – ARC-Lake</p>	<p>Document Ref: ARC-Lake-ATBD-v1.3 Issue: 1 Date: 23 Oct 2013</p>
---	---	--

ATSR Reprocessing for Climate Lake Surface Water Temperature: ARC- Lake

Algorithm Theoretical Basis Document

The University of Edinburgh 	ATSR Reprocessing for Climate Lake Surface Water Temperature – ARC-Lake	Document Ref: ARC-Lake-ATBD-v1.3 Issue: 1 Date: 23 Oct 2013
---	--	--

Title: ATSR Reprocessing for Climate Lake Surface Water Temperature: ARC-Lake:
Algorithm Theoretical Basis Document


Document Number: ARC-Lake-ATBD-v1.3


Issue: 1

Revision: 1.3

Date: 23 November 2013


Signature Table

	Name	Function	Company	Signature	Date
Prepared	S MacCallum	Researcher	University of Edinburgh		23 October 2013
	C Merchant	PI/Professor	University of Reading		
Approved					
Released					

The University of Edinburgh 	ATSR Reprocessing for Climate Lake Surface Water Temperature – ARC-Lake	Document Ref: ARC-Lake-ATBD-v1.3 Issue: 1 Date: 23 Oct 2013
---	--	--

Document Change Record

Version	Date	Author	Description
1.0	8 Oct 2010	SM, CM	
1.1	1 Nov 2011	SM, CM	Updated to reflect changes in methodology and terminology between v1.0 and v1.1 data products
1.2	22 Nov 2011	SM, CM	Updated to reflect changes in methodology: addition of ATSR1, 2010, and changes to estimation of prior LSWT
1.3	23 Oct 2013	SM, CM	Updated to reflect addition of AATSR, 2011 for v2.0 data products.

<p>The University of Edinburgh</p> 	<p>ATSR Reprocessing for Climate Lake Surface Water Temperature – ARC-Lake</p>	<p>Document Ref: ARC-Lake-ATBD-v1.3 Issue: 1 Date: 23 Oct 2013</p>
---	---	--




<p>The University of Edinburgh</p> 	<p>ATSR Reprocessing for Climate Lake Surface Water Temperature – ARC-Lake</p>	<p>Document Ref: ARC-Lake-ATBD-v1.3 Issue: 1 Date: 23 Oct 2013</p>
--	--	--

Table of Contents

1	INTRODUCTION	8
1.1	Acronyms and Abbreviations	8
1.2	Purpose and Scope	10
1.3	Algorithm Identification	10
2	ALGORITHM OVERVIEWS	11
2.1	Identification of lakes	11
2.2	Lake-specific inputs to radiative transfer modelling (simulation)	11
2.3	Classification	12
2.4	Lake Surface Water Temperature retrieval	12
2.5	Gridding	12
3	IDENTIFICATION OF LAKES	13
3.1	Description algorithm and justification	13
3.2	Practical considerations	14
3.3	Assumptions and limitations	15
4	LAKE-SPECIFIC PRIOR SURFACE TEMPERATURE	16
4.1	Initialization with MODIS Climatology	16
4.2	Iterative Scheme for Generating Prior Surface Temperature for ARC-Lake	17
4.3	Sources of prior and availability of reconstructed time series	22
4.4	Implementation of high resolution prior surface temperature field	22
5	LAKE-SPECIFIC EMISSIVITY	24
6	BAYESIAN CLEAR-SKY PROBABILITY	26
6.1	Bayesian Probability Theory	26


<p>The University of Edinburgh</p> 	<p>ATSR Reprocessing for Climate Lake Surface Water Temperature – ARC-Lake</p>	<p>Document Ref: ARC-Lake-ATBD-v1.3 Issue: 1 Date: 23 Oct 2013</p>
--	--	--

6.2	Probability density functions – clear-sky	27
6.2.1	Definitions	27
6.2.2	Definitions	28
6.2.3	LSD Distributions	30
6.3	Probability density functions – cloudy-sky	30
6.3.1	Definitions	30
6.3.2	Joint BT Distributions	31
6.3.3	LSD Distributions	34
6.4	Clear-sky Probability	35
6.4.1	Unconditional clear-sky probability - $P(c)$	35
6.4.2	Conditional clear-sky probability - $P(c \mathbf{y}^o, \mathbf{x}^b)$	35
6.5	Practical considerations	36
7	ICE IN PIXEL TEST	37
8	LAKE SURFACE WATER TEMPERATURE RETRIEVAL WITH UNCERTAINTY	39
8.1	Optimal Estimation (OE) Retrievals	39
8.2	Treatment of Uncertainties	41
8.2.1	Introduction	41
8.2.2	Systematic Errors	41
8.2.3	Random Errors (Uncertainty Estimate)	43
8.2.4	Other Errors	46
8.2.5	Confidence Indicators	46
9	GRIDDING	48
10	ATSR-1 MODIFICATIONS	50
11	OTHER SOURCES OF INFORMATION	51
12	REFERENCES	52
13	APPENDIX	55
13.1	Sources of data for prior LSWT field	55

<p>The University of Edinburgh</p> 	<p>ATSR Reprocessing for Climate Lake Surface Water Temperature – ARC-Lake</p>	<p>Document Ref: ARC-Lake-ATBD-v1.3 Issue: 1 Date: 23 Oct 2013</p>
--	--	--

List of Figures


Figure 1. Flow-chart describing iterative processed used to generate high resolution prior LSWT field.	21
Figure 2. Clear-sky 11 μm textural PDF for night-time AATSR.	30
Figure 3. Examples of slices of the night-time cloudy-sky spectral PDF LUT for AATSR. All figures illustrate the LUT used for the nadir view for a prior LSWT range of 280.0 K to 282.5 K. (a) 11 μm - SST vs 11 μm - 12 μm for 3.7 μm - 11 μm differences of 2.0 K to 2.2 K. (b) 11 μm - SST vs 3.7 μm - 11 μm for 11 μm - 12 μm differences of 4.0 K to 4.2 K. . (c) 11 μm - 12 μm vs 3.7 μm - 11 μm for 11 μm - SST differences of -6.0 K to -4.0 K.	32
Figure 4. Examples of slices of the day-time cloudy-sky spectral PDF LUT for AATSR. All figures are illustrative for a prior SST range of 280.0 K to 282.5 K and 11 μm - SST differences of -6.0 K to -4.0 K. (a) 11 μm nadir - 11 μm forward vs 11 μm nadir - 12 μm nadir for 11 μm forward - 12 μm forward differences of 3.0 K to 3.4 K. (b) 11 μm nadir - 11 μm forward vs 11 μm forward - 12 μm forward for 11 μm nadir - 12 μm nadir differences of 3.0 K to 3.4 K. (c) 11 μm forward - 12 μm forward vs 11 μm nadir - 12 μm nadir for 11 μm nadir - 11 μm forward differences of 3.0 K to 3.4 K.	33
Figure 5. Example slice of cloudy-sky spectral PDF LUT for 1.6 μm day-time for solar zenith angles in the range 55° to 57.5°.....	34
Figure 6. Cloudy-sky 11 μm textural PDF for night-time AATSR.....	35

<p>The University of Edinburgh</p> 	<p>ATSR Reprocessing for Climate Lake Surface Water Temperature – ARC-Lake</p>	<p>Document Ref: ARC-Lake-ATBD-v1.3 Issue: 1 Date: 23 Oct 2013</p>
--	--	--

1 INTRODUCTION

1.1 Acronyms and Abbreviations

<i>AATSR</i>	<i>Advanced ATSR</i>
<i>ARC</i>	<i>ATSR Reprocessing for Climate</i>
<i>ATBD</i>	<i>Algorithm Theoretical Basis Document</i>
<i>ATSR</i>	<i>Along-Track Scanning Radiometer</i>
<i>BT</i>	<i>Brightness Temperature</i>
<i>DINEOF</i>	<i>Data Interpolating Empirical Orthogonal Functions</i>
<i>DISORT</i>	<i>Discrete Ordinates Radiative Transfer Program for a Multi-Layered Plane-Parallel Medium</i>
<i>GLWD</i>	<i>Global Lakes and Wetlands Database</i>
<i>LIC</i>	<i>Lake Ice Concentration</i>
<i>LSWT</i>	<i>Lake Surface Water Temperature</i>
<i>LUT</i>	<i>Look-Up Table</i>
<i>MAP</i>	<i>Maximum A posteriori Probability</i>
<i>MODIS</i>	<i>Moderate Resolution Imaging Spectroradiometer</i>
<i>NEAT</i>	<i>Noise Equivalent Differential Temperature</i>
<i>NIR</i>	<i>Near Infra-Red</i>
<i>NWP</i>	<i>Numerical Weather Prediction</i>
<i>OE</i>	<i>Optimal Estimation</i>
<i>PDF</i>	<i>Probability Density Function</i>
<i>RFM</i>	<i>Reference Forward Model</i>
<i>RMSD</i>	<i>Root-Mean-Square Deviation</i>
<i>RT</i>	<i>Radiative Transfer</i>
<i>RTM</i>	<i>Radiative Transfer Model</i>

<p>The University of Edinburgh</p> 	<p>ATSR Reprocessing for Climate Lake Surface Water Temperature – ARC-Lake</p>	<p>Document Ref: ARC-Lake-ATBD-v1.3 Issue: 1 Date: 23 Oct 2013</p>
---	---	--

RTTOV *Radiative Transfer for TOVs (a fast RTM)*


SD *Standard Deviation*

SST *Sea Surface Temperature*

TCWV *Total Column Water Vapour*

TIR *Thermal Infra-Red*

ToA *Top of Atmosphere*

<p>The University of Edinburgh</p> 	<p>ATSR Reprocessing for Climate Lake Surface Water Temperature – ARC-Lake</p>	<p>Document Ref: ARC-Lake-ATBD-v1.3 Issue: 1 Date: 23 Oct 2013</p>
--	--	--

1.2 Purpose and Scope

This document is an Algorithm Theoretical Basis Document for the generation of Lake Surface Temperature (LSWT) and Lake Ice Concentration (LIC) products from Along-Track Scanning Radiometer (ATSR) imagery.


Such products have not been adequately delivered by previous systems developed for either sea surface temperature or land surface temperature determination. However, there is a need for LSWT and LIC for many applications: numerical weather prediction is the most pressing application, since increasing spatial resolution and sophistication of surface-atmosphere interactions in weather simulations no longer permits that lakes are neglected or very crudely represented; other applications include climate monitoring, limnological research, and climate prediction for commercial and societal institutions.

In terms of scope, this ATBD covers ATSR-1, ATSR-2 and Advanced ATSR (AATSR) processing.

1.3 Algorithm Identification

The ATBD provides the theoretical basis for the following algorithms:

- identification of image pixel locations covering required “large lakes” (which are defined)
- determination of lake-specific inputs required for radiative transfer modelling (the radiative transfer models are not part of the ATBD, since the algorithms are independent of these)
- discrimination of cloudy and non-cloudy pixels, and of water and ice clear-sky pixels (“classification”)
- estimation of LSWT, uncertainty in LSWT for clear-sky pixels
- conversion of pixel observations to a gridded product

<p>The University of Edinburgh</p> 	<p>ATSR Reprocessing for Climate Lake Surface Water Temperature – ARC-Lake</p>	<p>Document Ref: ARC-Lake-ATBD-v1.3 Issue: 1 Date: 23 Oct 2013</p>
--	--	--

2 ALGORITHM OVERVIEWS

2.1 Identification of lakes


The algorithms are designed to support production of LSWT and LIC for large lakes. Large lakes are commonly defined as natural inland water bodies of $>500 \text{ km}^2$ in surface area (Herdendorf (1982), Beeton (2002)). In addition, the target lakes for the ARC-Lake project include some inland waters that are less than 500 km^2 in area (because ARC-Lake users have requested these, or because there are useful validation data available).

The lake identification algorithm determines, on the basis of the longitude and latitude of a pixel in the ATSR level 1b imagery, whether that pixel is geolocated over a target lake, and, if so, which lake is in view. This is done on the basis of a hierarchical temporally fixed lake mask. Being temporally fixed, ephemeral lakes are not included in the target lake list, and lakes undergoing dramatic hydrological changes are not properly accounted for in this version of the algorithm.

2.2 Lake-specific inputs to radiative transfer modelling (simulation)

The classification and retrieval algorithms discussed in §6 and §8 are based on radiative transfer modelling. The algorithms are generic with respect to what choice of radiative transfer model (RTM) is applied, so long as appropriate simulations of brightness temperature (BT) and visible reflectance, can be made. In addition, the jacobian (derivative of BT) is required with respect to prior surface temperature (x^b) and prior total column water vapour (w^b); any radiative transfer model that simulates BT can provide the jacobians by perturbation if it does not directly output them. Thus, discussion of the RTMs as such is properly outside the scope of this ATBD. Likewise, the algorithms are generic with respect to the origin of the profiles of atmospheric temperature and water vapour that are required to run the RTM: the sourcing of such numerical weather prediction (NWP) fields for a given location and observation is a generic process for which any implementer of ARC-Lake algorithms will have a preferred local solution.

However, the sourcing of the prior surface temperature, x^b , and the lake surface emissivity, ϵ , are also required, and we have found that NWP-based values for these are not (at present) sufficiently accurate for use in ARC-Lake. Therefore, they need to be specified by an algorithm, presented here. The x^b algorithm is simple: it involves looking up pre-calculated data giving a spatially complete field of prior surface temperature for the period 1995 to 2009. This ATBD is therefore focussed on documenting the basis for those look-up data. The emissivity algorithm involves interpolation of fresh and saline water emissivity according to the nature of any given lake.

<p>The University of Edinburgh</p> 	<p>ATSR Reprocessing for Climate Lake Surface Water Temperature – ARC-Lake</p>	<p>Document Ref: ARC-Lake-ATBD-v1.3 Issue: 1 Date: 23 Oct 2013</p>
--	--	--

2.3 Classification

Valid LSWT can be estimated only for pixels that are effectively clear-sky (free of cloud). The algorithm for assigning a probability of clear-sky to each pixel is based on Bayes' theorem (Merchant *et al*, 2005), and exploits the BT and visible simulations.

The LIC value for a cell is based on the fraction of clear-sky pixels in a cell that also triggers an ice detection algorithm.


2.4 Lake Surface Water Temperature retrieval

The LSWT is estimated for each clear-sky water pixel using joint optimal estimation (OE) of x^b and w^b given the simulations and observations. The form of optimal estimation used is to return the *maximum a posteriori probability* (MAP) assuming Gaussian error characteristics.

OE also gives an uncertainty estimate for each retrieval.

2.5 Gridding

The lake products are required on a 0.05° latitude-longitude grid, and thus a gridding algorithm is specified, to take the observations from the imagery resolution to the product resolution.

<p>The University of Edinburgh</p> 	<p>ATSR Reprocessing for Climate Lake Surface Water Temperature – ARC-Lake</p>	<p>Document Ref: ARC-Lake-ATBD-v1.3 Issue: 1 Date: 23 Oct 2013</p>
--	--	--

3 IDENTIFICATION OF LAKES

3.1 Description algorithm and justification

A key component of the ARC-Lake processing system is the land/water mask, used to define the locations of lakes, and therefore locations where Lake Surface Water Temperature (LSWT) and Lake Ice Cover (LIC) should be derived. As we wish to treat each lake as a single entity, the land/water mask must also allow (A)ATSR observations to be attributed to a particular lake. Following assessment of existing land water masks, a new land/water mask was developed specifically for the lakes defined in Phase one of ARC-Lake (MacCallum and Merchant, 2010). Details of this development process follow.


The Envisat ATSR land/water mask (used operationally) was compared with the NAVOCEANO mask (GHRST, 2006). A summary of these two masks is given in Table 1. Although it does not provide full latitudinal coverage, the NAVOCEANO mask was preferred to the Envisat mask as it suffered fewer problems with missing or mis-located lakes. It also has the benefit of being at a higher resolution, allowing better representation of shorelines, and the potential advantage of containing information about the distance of each cell from the shore. Although not currently utilised, this information could be used to aid screening of land contaminated cells.

Mask	Resolution (degrees)	Latitude Coverage	Mask type	Number of lakes with no water cells
Envisat	0.01	[-90,90]	Binary	10
NAVOCEANO	0.00833	~[-80,80]	Distance from shore	3

Table 1. Summary of land/water masks assessed in ARC-Lake.

A problem shared by both the NAVOCEANO and Envisat ATSR masks is the lack of means by which to attribute water cells *to a particular lake*. Due to the irregular shapes of lakes and the close proximity of other water bodies (e.g. other lakes, rivers, and oceans), it is not possible to do this by simply selecting a regular-shaped area surrounding the location of the lake centre. It is also not possible to define the cells for a given lake as the group of connecting water cells overlying the location of the lake centre, as areas of some lakes (e.g. Lake Astray) are smaller than the resolution of the mask, and therefore the lakes (although fully connected in reality) may consist of groupings of non-connecting cells. This problem of correctly attributing water cells in the mask to specific lakes was tackled by incorporating a polygon definition of each lake.

The Global Lakes and Wetlands Database, GLWD (Lehner and Döll, 2004), describes each lake as a polygon. These polygons consist of an array of longitude/latitude coordinates

<p>The University of Edinburgh</p> 	<p>ATSR Reprocessing for Climate Lake Surface Water Temperature – ARC-Lake</p>	<p>Document Ref: ARC-Lake-ATBD-v1.3 Issue: 1 Date: 23 Oct 2013</p>
--	--	--


defining the main shoreline of the lake and the shorelines of islands within the lake. Lehner and Döll (2004) derive these polygons from the Digital Chart of the World (DCW) of ESRI (1993), with manual adjustments made to define boundaries between the lakes and other water bodies. A new land/water mask (GLWD mask) at the NAVOCEANO resolution was generated from these polygons, with cells being flagged as water only if they were completely land free (i.e. entirely enclosed by the lake shoreline polygon and not intersected/contaminated by any island polygons). Unlike the Envisat and NAVOCEANO masks that only distinguish between land and water, the new GLWD mask distinguishes between individual lakes by flagging water cells with a unique lake identifier number.

As a conservative approach, the NAVOCEANO and GLWD masks were combined to create the ARC-Lake land/water mask. Only cells flagged as water in both masks were defined as water in the new mask, giving a conservative representation of the water cells comprising each lake. In the special cases where the NAVOCEANO mask contained no water cells for the lake (e.g. Lake Hazen), the GLWD mask was used. The result of this process is a global (including the high latitudes) land/water mask at a grid resolution of 0.00833° , where each of the Phase one lakes is represented by a unique number.

3.2 Practical considerations

The lakes covered Phase one of ARC-Lake, and indeed all lakes, only cover a small fraction of the Earth's surface. Therefore compression techniques are applied to reduce the memory storage requirements of the mask. The mask is stored in a hierarchical data structure, with three levels of increasing resolution as detailed in Table 2. By storing only the full resolution mask for 0.1° resolution cells that contain lakes, the hierarchical data structure greatly reduces the storage requirements for this mask. The land/water mask is available in NetCDF format from an online data repository (MacCallum and Merchant, 2011c).

Level	Resolution	Dimensions	Details
1	$1.0^\circ \times 1.0^\circ$	[360, 180]	<p>0 - No lake data</p> <p>> 0 - Index (n) of 2nd dimension of Level 2 (indexing starts at 1, i.e. F90 standard)</p> <p>Number of non-zero elements = N = size of 2nd dimension of Level 2</p>
2	$0.1^\circ \times 0.1^\circ$	[100, N]	<p>0 - No lake data</p> <p>> 0 - Index (m) of 2nd dimension of Level 3 (indexing starts at 1, i.e. F90 standard)</p> <p>Number of non-zero elements = M = size of 2nd dimension of Level 3</p>

<p>The University of Edinburgh</p> 	<p>ATSR Reprocessing for Climate Lake Surface Water Temperature – ARC-Lake</p>	<p>Document Ref: ARC-Lake-ATBD-v1.3 Issue: 1 Date: 23 Oct 2013</p>
--	--	--

3	0.01° x 0.01°	[100, M]	0 - No lake data > 0 - ARC-Lake index number for lake
---	---------------	----------	--


Table 2. Structure of hierarchical land/water mask developed for ARC-Lake.

3.3 Assumptions and limitations

The new land/water mask outlined in §3.2 is generated only for the lakes defined in Phase one of the ARC-Lake project (MacCallum and Merchant, 2010). This set of target lakes contains water bodies broadly described as permanent, natural water bodies with surface area > 500 km², with a number of exclusions and additions (MacCallum and Merchant, 2010). One such exclusion is lakes with highly variable surface area (> 25%). Such lakes are not included to avoid the issue of LSWT retrievals being performed over land when the lakes recede. There are however still lakes where lesser (or undocumented) variations in surface area occur. Therefore it should be noted that land contamination may still be an issue around lake edges.

There are also two lakes (the Aral Sea and Kara-Bogaz-Gol) where significant changes to the surface area have occurred over the lifetime of the ATSR missions, rather than seasonally. In these cases, the land/water mask represents the lake extent at a snap-shot in time, so therefore does not accurately represent the lake area throughout the ATSR mission lifetime. Consequently, LSWT products for these lakes should be used with caution.

The problem of variations in lake surface area is one that must be addressed in future. A water detection algorithm based on visible reflectance channel observations is proposed, and will be trialled in Phase 3 of the ARC-Lake project (months 27 to 36) in the context of extending the range target lakes within the project to smaller inland water bodies.

<p>The University of Edinburgh</p> 	<p>ATSR Reprocessing for Climate Lake Surface Water Temperature – ARC-Lake</p>	<p>Document Ref: ARC-Lake-ATBD-v1.3 Issue: 1 Date: 23 Oct 2013</p>
--	--	--

4 LAKE-SPECIFIC PRIOR SURFACE TEMPERATURE


The prior surface temperature is a key component of the optimal estimation (OE) LSWT retrieval scheme implemented in ARC-Lake. NWP-based values, as used in sea surface temperature (SST) retrievals, are not (at present) adequate for use in ARC-Lake. The reasons for this are two-fold: the NWP-based values are not accurate enough and their spatial resolution too coarse to provide information of spatial thermal structures on lake-scales. This is particularly apparent for smaller or less well monitored lakes. It is therefore necessary to specify the prior surface temperature by other means. These means take the form of an iterative scheme, using the ARC-Lake LSWT product to generate a spatially and temporally complete field of surface temperatures by means of principal component reconstruction, that are then used as the input field for the next run of the ARC-Lake processor.

4.1 Initialization with MODIS Climatology

In many instances (e.g., for ECMWF and Met Office), NWP surface temperature over lakes is provided by prescribing a monthly climatology value, for example, based on nearby sea surface temperatures (Saunders and Basalmo, personal communications). As NWP-based values are therefore insufficiently accurate and at a resolution too coarse for ARC-Lake LSWT retrievals over many lakes an alternative initial prior temperature field was sought. This was necessary in order to limit the number of potentially valid observations flagged as cloud because of very large differences between the prior and the retrieval. SST and land surface temperature (LandST) retrievals from the Moderate Resolution Imaging Spectroradiometer (MODIS) were deemed to be a potentially suitable alternative to NWP, as they have been applied with some success to lakes from 2000 to present (Oesch *et al*, 2005, Reinart and Reinhold, 2008, and Wan *et al*, 2008) and are available at a finer resolution than NWP data ($\sim 1/20^\circ$ compared to $\sim 1.0^\circ$).

Although monthly temporal resolution may result in the loss of information about short-lived thermal fronts, it was both feasible to achieve this and was deemed adequate for the creation of prior LSWT fields for the first iteration. Monthly climatology from MODIS SST products (which operate over all identified water bodies) were used, with MODIS LandST products being used for lakes where SST products were unavailable (because the MODIS SST algorithm had not been applied), in order to maximise the coverage of the target lakes.

Terra MODIS SST (11 μm day-time and night time) monthly climatology products, at $1/24^\circ$ longitude/latitude resolution, were obtained from <http://oceancolor.gsfc.nasa.gov> (MODIS, 2010). Equivalent climatology products were not available for MODIS LandST, so these were generated from monthly average files (MOD11C3) downloaded from <https://lpdaac.usgs.gov> (Wan, 2007). MODIS LandST products are on $1/20^\circ$ longitude/latitude resolution.

<p>The University of Edinburgh</p> 	<p>ATSR Reprocessing for Climate Lake Surface Water Temperature – ARC-Lake</p>	<p>Document Ref: ARC-Lake-ATBD-v1.3 Issue: 1 Date: 23 Oct 2013</p>
--	--	--


A global MODIS Lake Surface Water Temperature (LSWT) climatology at $1/8^\circ$ resolution was created, as a composite of the SST and LandST products, using the ARC-Lake land/water mask (MacCallum and Merchant, 2010) to define lake cells. Data were not available in all temperature products (SST/LandST, day/night) for all lake cells and in some cases data was unavailable in all products. Where available, MODIS day-time SST was used. If these data were not present, the MODIS night time SST product was used. If no SST data were present for a given lake, a lake-area-average LandST value was used, with preference to the day-time product if available. As fine resolution spatial features such as thermal fronts may persist for shorter timescales than this climatology, there is some redundancy in using the MODIS products at their full resolution at this stage. Therefore, the MODIS products were spatially averaged to a $1/8^\circ$ resolution grid to further maximise spatial coverage and reduce processing time.

Interpolation from surrounding LSWTs is used to fill lake cells or lakes that have missing data. This interpolation stage is performed in the ARC-Lake processing code to provide a spatially complete input field. Linear interpolation between monthly time steps is used to determine the prior LSWT field for a given day of the year.

4.2 Iterative Scheme for Generating Prior Surface Temperature for ARC-Lake

The climatology for each lake developed from MODIS is useful for providing a reasonable prior for some of the smaller lakes, but does not provide the temporal and spatial resolution necessary to correctly represent the how lake temperatures vary in time and in space across a given lake. Nor does it capture any inter-annual variability, of course. It was therefore adequate for an initial run of the ARC-Lake processor, but is not capable of giving best results. A better prior (with adequate temporal and spatial resolution, and with inter-annual variability present where possible) was therefore developed by an iterative approach as described in this section.

The climatology derived from MODIS was used as input to the ARC-Lake processor, and some valid observations of LSWT were obtained. A prior LSWT field of the spatial and temporal resolution necessary for an improved result was then achieved by applying data-interpolating principal component techniques (Alvera-Azcárate, 2005) to these satellite observations of LSWT. This allows gaps in the LSWT data, arising from cloud cover and incomplete lake coverage in the instrument swath, to be filled in space, thereby providing complete spatial coverage on each day of observation. These fields were then linearly interpolated in time to yield a spatially complete LSWT time series for every day of the year during the ATSR2 and AATSR missions (in most cases – see below). Since the interpolation process creates fields with errors that are uncorrelated or very weakly correlated to LSWT retrieval errors, the complete time series may be fed back into the retrieval scheme as a prior LSWT, and the process repeated, with improved results, particularly in terms of cloud

<p>The University of Edinburgh</p> 	<p>ATSR Reprocessing for Climate Lake Surface Water Temperature – ARC-Lake</p>	<p>Document Ref: ARC-Lake-ATBD-v1.3 Issue: 1 Date: 23 Oct 2013</p>
---	---	--


detection. Figure 1 illustrates this iterative process, the components of which are described in the following sections.

There are three key components to this iterative processing scheme: the ARC-Lake processor for LSWT, software for reconstructing a spatially complete LSWT field from the ARC-Lake output using empirical orthogonal function (EOF)-based techniques, and a lake model. The ARC-Lake processor is described in this document and the references herein. The EOF decomposition based reconstructions of the spatially incomplete output from the ARC-Lake processor are generated using the software package, DINEOF (Data Interpolating Empirical Orthogonal Functions). This software, described in detail by Alvera-Azcárate (2005), allows missing data points (e.g. clouds and areas not under the instrument swath) in the ARC-Lake LSWT product to be calculated from an optimal number of EOFs determined using a cross-validation technique. Finally, output from the lake model, FLake (Mironov, 2005) is used for cases where the number of valid observations from ARC-Lake is extremely low and/or the EOF reconstruction is poor. It is also used to enhance the representation of frozen periods, which may suffer from problems of extensive cloud cover and of surface ice being flagged as cloud by the ARC-Lake processor. The simplified online version of FLake is used (<http://www.flake.igb-berlin.de/>) which provides an approximation to a climatic mean temperature cycle. It is beyond the scope of this document to explain the workings of DINEOF or Flake in further detail and the user is directed to the references given. The iterative processing scheme for generating and using the prior LSWT field is outlined in Figure 1 and described below.

Per-lake output products (as described in MacCallum and Merchant, 2011a) from the ARC-Lake processor are the starting point for the process that ultimately creates a global prior LSWT fields at daily resolution that are then used as input to the ARC-Lake processor in the next iteration (except for the first pass, where the climatology based on MODIS observations was used). Cloud cover and orbit tracks prevent the ARC-Lake LSWT product providing spatially complete observations over each lake at every opportunity. Alvera-Azcárate (2005) demonstrate that these data gaps can be filled using EOF-based reconstructions. Before running DINEOF a number of preprocessing steps are required to remove erroneous observations that may adversely affect the reconstructions, and to ensure that there are adequate observations to perform the reconstruction.

Erroneous outliers in the input LSWT field (e.g. from land contamination) can result in unrealistic features being propagated through the reconstruction. To eradicate this problem, the input LSWT data are filtered by their χ^2 value (the OE retrieval cost), with all points with $\chi^2 > 100$ flagged as missing data.

During periods where temperatures are approach freezing or are frozen, long periods with no valid LSWT observations or detected ice cover occur over some lakes. To avoid unrealistic temperatures over these periods, missing data points are replaced by FLake simulations in the

<p>The University of Edinburgh</p> 	<p>ATSR Reprocessing for Climate Lake Surface Water Temperature – ARC-Lake</p>	<p>Document Ref: ARC-Lake-ATBD-v1.3 Issue: 1 Date: 23 Oct 2013</p>
---	---	--


reconstructed/interpolated time series. As the FLake simulations approximate to a climatic mean over the entire lake, they do not capture seasonal or spatial variations in ice cover. Consequently, a more conservative estimate of the frozen period is taken to avoid unrealistic switches between frozen and unfrozen conditions across the lake and in the reconstructed time series. The conservative estimate of the frozen period adopted is the central 60% of the frozen period simulated in FLake. All potential (but cloud or ice covered) observations during this period are replaced with the value 273.15 K.

The methodology above is updated for the prior LSWT for v2.0. Following the updates made to the ice detection algorithm in v1.1 (to reduce the possibility of thin cirrus being flagged as ice) the LIC product is integrated into prior LSWT field for v2.0. All cells containing ice observations but no valid LSWT observations are replaced with the value 273.15 K prior to the substitution of FLake simulations. This provides improved representation of ice cover and LSWT during freeze/thaw periods and reduces the influence of FLake simulations on the prior LSWT field. Note that ice detection is only performed during the day (§7), as it uses visible channel observations. To avoid losing the benefits of the ice observations in the night-time reconstructions, day-time ice observations are substituted into the night-time LSWT observations (as above), only days where there is both a day and night-time observation.

Alvera-Azcárate (2005) demonstrate that EOF-based reconstructions perform best when each temporal slice of data (each day) has valid data for at least 5% of the potential points. A filter is applied to the data based on this criterion. Following this, a check is made on the number of remaining time-steps of data relative to the total number of potential observation days. If more than 15% of the time-steps have valid observations the algorithm proceeds with this data. However, if there are fewer time steps than this, a daily climatology for an average year is constructed from all the available data, and this single year time series used as input to DINEOF. It should be noted that days where FLake simulations have been substituted in are excluded from this filtering stage.

A spatially complete time series (covering observation days only) is then generated using DINEOF (Alvera-Azcárate, 2005). This is used to further filter the original input LSWT field to remove remaining outliers. Observation-reconstruction differences are calculated for all valid observations. Where this difference is greater than 2.5 times the standard deviation over all differences, the LSWT observation is replaced with the reconstructed temperature.

Following the second stage of filtering a second reconstruction is generated using DINEOF. This reconstruction is then linearly interpolated in time to provide a spatially and temporally complete time series of LSWT for each lake. Lake cells with no valid observations result in missing data in the reconstruction. Such cells are replaced by the median of the surrounding cells, where the size of the median filter applied is variable, to ensure a minimum of 5 cells are used. Occasional unrealistic spatial and temporal variations in temperature may still be

<p>The University of Edinburgh</p> 	<p>ATSR Reprocessing for Climate Lake Surface Water Temperature – ARC-Lake</p>	<p>Document Ref: ARC-Lake-ATBD-v1.3 Issue: 1 Date: 23 Oct 2013</p>
--	--	--

present in the reconstructions. These are removed by applying median filters in space (as above) and in time (with a width of 15 to ensure ~5 observations are used).

Manual checks are performed at this stage: comparing the time series of lake-mean reconstructed LSWTs with the lake-mean observation. The purpose of these checks is to determine whether the reconstruction is realistic or whether the FLake simulation is a more suitable prior. FLake simulations are used as a last resort for cases where the reconstructions are in poor agreement with observations, typically cases where the observations are extremely sparse. Where DINEOF reconstructions are of good quality, day and night time reconstructions are averaged to provide a single time series for each instrument. Only a single reconstruction is used if only one of the day/night pair is of suitable quality,

Reconstructions for all the Phase one lakes are then merged to create daily files with global coverage at a resolution of $1/20^\circ$. An estimate of the error in the prior LSWT field is also required. For lakes where FLake is used as the prior, the error (SD) is assigned to 2.0 K. For lakes where the DINEOF reconstruction is used, the error estimate is taken from the comparison of the prior from the previous iteration with *in situ* observations in the MD (MacCallum and Merchant, 2010). These daily global files of reconstructed and modelled LSWTs with associated error estimates are then used as the prior LSWT field in the next run of the ARC-Lake processor and the process, as outlined above and in Figure 1, repeats iteratively. As illustrated in Figure 1 the full time series of observations for each instrument is used as input to the iterative scheme.

A modified approach is used for ATSR-1 and additional AATSR observations (e.g. 2010 and 2011). For efficiency, we use the ATSR-2/AATSR climatology from v1.1 products (rather than MODIS climatology) as the initial prior LSWT, with a fixed error estimate of 2 K. Following this initialisation run, one further iteration of the processing scheme (Figure 1) is performed to generate the v2.0 data products for ATSR-1 and 2010-2011 (AATSR). Two further modifications are made to the ATSR-1 processing. Firstly, no visible channels are available on ATSR-1 and therefore no ice cover observations (§7) are possible during the day or night. To reduce dependence on FLake simulations, we substitute in frozen periods based on ATSR-2/AATSR climatology before generating the reconstructions. This is done by replacing potential but missing observations with value 273.15 for cells/dates where the ATSR-2/AATSR climatology is < 273.4 K (the additional 0.25 K is to accommodate deviations from frozen that can occur in the reconstructions). Secondly, for lakes where a lack of ATSR-1 observations prevents the generation of a full time-series reconstruction the ATSR-2/AATSR climatology is used, as this generally provides a more realistic representation of the seasonal cycle.

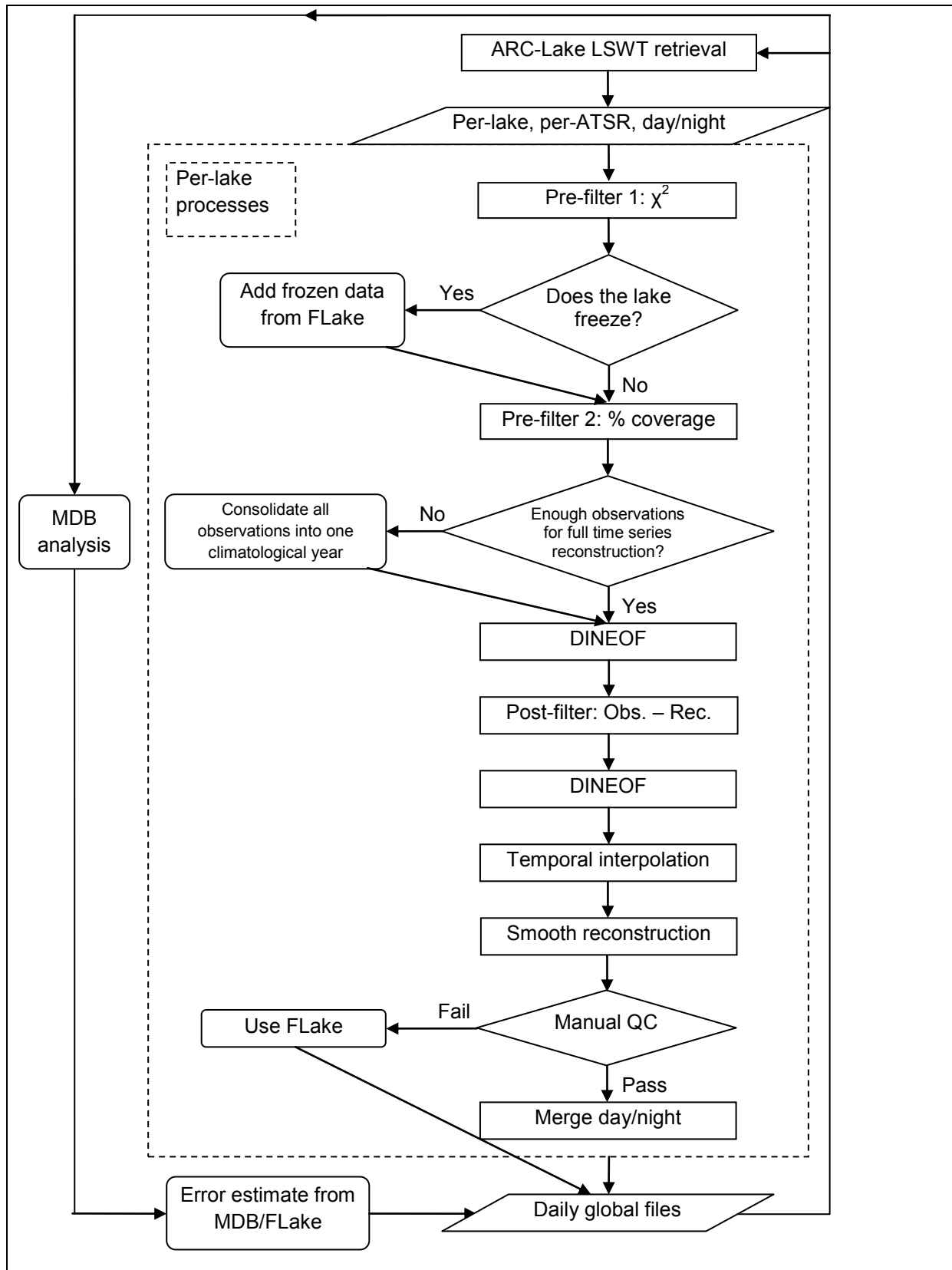



Figure 1. Flow-chart describing iterative processes used to generate high resolution prior LSWT field.

<p>The University of Edinburgh</p> 	<p>ATSR Reprocessing for Climate Lake Surface Water Temperature – ARC-Lake</p>	<p>Document Ref: ARC-Lake-ATBD-v1.3 Issue: 1 Date: 23 Oct 2013</p>
--	--	--

4.3 Sources of prior and availability of reconstructed time series


As outlined in §4.2, the final time series of LSWT used as input in the ARC-Lake processor come from one of three possible sources (in order from most to least preferred): DINOEF reconstructions of the full instrument time series, DINEOF reconstructions of daily climatology, or FLake simulations. With each iteration it is found that the number of lakes where the prior comes from the more preferred sources increases. In generating the version 1.0 release of ARC-Lake, two iterations were undertaken. A third iteration was performed in generating the version 1.1 release of ARC-Lake products. A fourth iteration was performed in generating the v2.0 ARC-Lake products. The number of lakes where the prior LSWT came from each of these sources (and combinations of them) for versions 1.0, 1.1 and 2.0 is given in Table 3. A detailed breakdown of the version 2.0 data in Table 3 is given in Table 4 in §13.

Version	Instrument	Reconstructed time series	Reconstructed climatology	Mix of reconstructions	FLake
1.0	ATSR2	81	135	22	25
	AATSR	112	112	17	22
1.1	ATSR2	126	97	28	12
	AATSR	160	73	16	14
2.0	ATSR1	112	113	34	4
	ATSR2	174	27	57	5
	AATSR	183	16	60	4

Table 3. Sources of data for prior LSWT field.

4.4 Implementation of high resolution prior surface temperature field


The OE retrieval scheme requires the input of prior meteorological fields and forward modelling based on these fields. As atmospheric fields are smooth compared to the spatial scales of LSWT variation, it is not necessary to perform the forward modelling at every satellite pixel or grid cell of a high resolution prior. Instead, forward modelling is carried out at ATSR tie-points (resolution $\sim 0.225^\circ$), using the distance weighted average of the four nearest neighbours from the high resolution LSWT prior. Due to computational limitations this transform to ATSR tie-points is performed on a reduced resolution (0.1°) version of the prior (generated from the 0.05° reconstruction). The full resolution (0.05°) prior is later

<p>The University of Edinburgh</p> 	<p>ATSR Reprocessing for Climate Lake Surface Water Temperature – ARC-Lake</p>	<p>Document Ref: ARC-Lake-ATBD-v1.3 Issue: 1 Date: 23 Oct 2013</p>
--	--	--

combined with the forward model output at tie-points to estimate the prior BTs at the higher resolution. This is achieved by bilinear interpolation of the quantity

$$\mathbf{F}(x_a) + \frac{\partial y}{\partial x}(x_{hi-res} - x_a)$$

which is then used as the forward model value for pixels corresponding to x_{hi-res} rather than $\mathbf{F}(x_a)$. Here: x_a is the prior LSWT on tie-points, x_{hi-res} is the high resolution LSWT prior, $\frac{\partial y}{\partial x}$ is the tangent linear of BTs with respect to surface temperature, and $\mathbf{F}(x_a)$ represents the forward modelled BTs for the state vector at the tie-points.

<p>The University of Edinburgh</p> 	<p>ATSR Reprocessing for Climate Lake Surface Water Temperature – ARC-Lake</p>	<p>Document Ref: ARC-Lake-ATBD-v1.3 Issue: 1 Date: 23 Oct 2013</p>
--	--	--

5 LAKE-SPECIFIC EMISSIVITY

Values of the infrared emissivity of water surfaces are another important component of the forward model, and require a spectral emissivity model to calculate them. Such a model must account for the emissivity variations associated with wavelength, view angle, wind speed, water temperature and, for the case of lake surfaces, salinity. A suitable emissivity model for ocean surfaces (neglecting salinity variations) is described by Embury et al. (2010), and is the basis of the lake-specific emissivity model used in ARC-Lake.

Embury et al. (2010) model the emissivity at any view angle using the following methods. They assume the water surface consisting of plane facets with a wind speed dependent slope distribution, calculate Fresnel reflection coefficients for each facet, and obtain the sum of their contributions (Masuda et al, 1988 and Masuda, 2006). In addition to the direct emission, Embury et al. (2010) also include a contribution from emitted radiation that has been reflected by the surface into the view angle (Watts et al. 1996, Wu and Smith 1997).


The isotropic Gaussian version of the clean surface slope distribution measured/modelled by Cox and Munk (1954) provides an appropriate description of the sea slope distribution (i.e., wind azimuth angle need not be considered). This distribution also provides an estimate of the background mean squared slope due to swell.

In order to avoid significant errors in simulated BTs the emissivity model must account for the temperature dependence of emissivity (Newman et al. 2005). This may be achieved through the use of temperature dependent values of refractive indices of water (pure and sea water). The refractive indices of Newman et al (2005) are recommended for the frequency range $760\text{--}1230\text{ cm}^{-1}$, and those of Downing et al (1975) elsewhere. Suitable treatment of the temperature dependence of the refractive indices is given by Newman et al (2005) for the range $760\text{--}1230\text{ cm}^{-1}$, and by Pinkley et al (1977) for other spectral regions. Temperature and salinity dependences may be assumed independent, and may be combined to calculate refractive indices for sea water (using a fixed standard value of 35 PSU) at different temperatures.

Embury et al.'s results are available at Filipiak (2008)

For the lake-specific emissivity model, refractive indices are also calculated for pure water and double sea water salinity (70 PSU) using the treatments of salinity dependence given by Pinkley and Williams (1976).

It is not necessary for the emissivity model to include the effect of surface foam, which will affect the emissivity at higher wind speeds. The effect of foam on the emissivity is likely to be smaller than the maximum effect proposed in Watts et al (1996), demonstrated by Salisbury et al (1993) who show emissivity is unaffected by foam in the $8\text{--}14\text{ }\mu\text{m}$ region. In

<p>The University of Edinburgh</p> 	<p>ATSR Reprocessing for Climate Lake Surface Water Temperature – ARC-Lake</p>	<p>Document Ref: ARC-Lake-ATBD-v1.3 Issue: 1 Date: 23 Oct 2013</p>
---	---	--

addition, the temperature of the foam may not match the skin temperature (Marmorino, 2005).

In the ARC-Lake processor, a salinity is associated with each lake ID. The forward model simulations then use an emissivity appropriate to that salinity obtained by linear interpolation of the emissivity for salinities of 0, 35, 70 PSU. This dependence upon salinity was introduced in ARC-Lake v1.1 data products (v1.0 products used a fixed salinity of 35 PSU for all lakes).

Limitations of this approach are as follows:

- The facet slope distribution with respect to wind speed used for emissivity calculations is appropriate to open ocean, and may not represent well situations of short fetch from lake shores.
- The relationship between NWP wind speed and local winds over a lake is likely to be less accurate than for the open ocean (because of topographical effects).
- A few lakes have salinity that varies spatially or in time to a significant degree, these variations not being represented by the single value used in the ARC-Lake processor.

<p>The University of Edinburgh</p> 	<p>ATSR Reprocessing for Climate Lake Surface Water Temperature – ARC-Lake</p>	<p>Document Ref: ARC-Lake-ATBD-v1.3 Issue: 1 Date: 23 Oct 2013</p>
--	--	--

6 BAYESIAN CLEAR-SKY PROBABILITY

The following sections describe the general principles of Bayesian probability theory and their application to cloud detection. It should be noted that all predefined probability density function look-up tables describing the distributions of cloudy radiances used in the ARC-Lake processing at present have been developed for SST observations rather than LSWT observations. To the degree that cloudy radiance distributions vary between land and sea, this gives scope for further improvement. Equivalent look-up tables based on ARC-Lake LSWT observations may be developed in the future, but this is not reckoned to be a priority, since cloud regimes vary significantly over the ocean in any case.

6.1 Bayesian Probability Theory

The problem being addressed is:

To deduce the likelihood of an image pixel being cloud-free given the radiance values from various thermal and reflectance channels for the pixel (and perhaps for other pixels in the image).

The radiance information can be supplemented with prior (background) knowledge. From the time and geographical location of the observations, climatological and/or NWP forecast values of surface temperature and atmospheric state can be specified. The addition of background information allows Bayesian statistics to be used to solve the problem posed.

Bayes' theorem for the probability of clear sky, c , given the observations, \mathbf{y}^o , and the background knowledge, \mathbf{x}^b , amounts to:

$$\text{Eq. 6.1} \quad P(c | \mathbf{y}^o, \mathbf{x}^b) = \frac{P(\mathbf{y}^o | \mathbf{x}^b, c)P(\mathbf{x}^b | c)P(c)}{P(\mathbf{y}^o | \mathbf{x}^b)P(\mathbf{x}^b)}$$

where each P represents a probability or probability density function as specified in its argument; c is the state of clear-sky clear-ocean; \mathbf{y} is the observation vector; \mathbf{x} is the state vector; superscript o indicates *observed* and superscript b indicates *background* (i.e., prior knowledge). The definition of the elements of the observation vector and background state will vary according to the sensor and forward model respectively.

For imagers used in meteorology, the clear-sky probability varies on length scales down to the pixel dimensions (~ 1 km). This is much finer than the length scales of variation in the atmospheric terms (other than cloudiness) in the background state (~ 100 km). To a good approximation on pixel-to-pixel scales, the background state is independent of clear-sky probability, that is $P(\mathbf{x}^b | c) = P(\mathbf{x}^b)$, simplifying Eq. 6.1 to

$$\text{Eq. 6.2} \quad P(c | \mathbf{y}^o, \mathbf{x}^b) = \frac{P(\mathbf{y}^o | \mathbf{x}^b, c)P(c)}{P(\mathbf{y}^o | \mathbf{x}^b)}$$

<p>The University of Edinburgh</p> 	<p>ATSR Reprocessing for Climate Lake Surface Water Temperature – ARC-Lake</p>	<p>Document Ref: ARC-Lake-ATBD-v1.3 Issue: 1 Date: 23 Oct 2013</p>
--	--	--

The term $P(\mathbf{y}^o | \mathbf{x}^b)$ describes the probability density function of the observations given the background state. We may decompose this probability density function into the contribution from clear and cloudy conditions, i.e.

$$\text{Eq. 6.3} \quad P(\mathbf{y}^o | \mathbf{x}^b) = P(c)P(\mathbf{y}^o | \mathbf{x}^b, c) + P(\bar{c})P(\mathbf{y}^o | \mathbf{x}^b, \bar{c})$$

where an over-bar signifies the logical *not* condition, and $P(\bar{c}) = 1 - P(c)$ by definition.

Substituting into Eq. 6.2 and rearranging gives the final form used to estimate the clear-sky probability:

$$\text{Eq. 6.4} \quad P(c | \mathbf{y}^o, \mathbf{x}^b) = \left[1 + \frac{P(\bar{c})P(\mathbf{y}^o | \mathbf{x}^b, \bar{c})}{P(c)P(\mathbf{y}^o | \mathbf{x}^b, c)} \right]^{-1}$$

Given a prior estimate of $P(c)$, evaluating the clear-sky probability in the light of the observations amounts to finding the probability density for the observations given the background state for both clear and cloudy conditions, and then using these values to evaluate Eq. 6.4

6.2 Probability density functions – clear-sky

6.2.1 Definitions


$P(\mathbf{y}^o | \mathbf{x}^b, c)$ is the probability of the observations given the background fields and assuming clear-sky. The observation vector, \mathbf{y}^o , consists of spectral and textural components. These are the channel brightness temperatures (or reflectances) and the local standard deviations of these, denoted by y_s^o and y_t^o respectively. It will be assumed that the local standard deviation PDFs are independent of the brightness temperatures (and reflectances), therefore for the clear probability:

$$\text{Eq. 6.1} \quad P(\mathbf{y}^o | \mathbf{x}^b, c) = P(\mathbf{y}_s^o | \mathbf{x}^b, c) \times P(\mathbf{y}_t^o | \mathbf{x}^b, c)$$

Using night-time AATSR retrievals as an example, the spectral component, \mathbf{y}_s^o , is composed of the brightness temperatures at 3.7 μm , 11 μm , and 12 μm , denoted by y_1 , y_2 , and y_3 . For the textural component, only the local standard deviation of the 11 μm brightness temperature is used, denoted by y_4 . Eq. 6.1 can therefore be written as:

$$\text{Eq. 6.2} \quad P(\mathbf{y}^o | \mathbf{x}^b, c) = P\left(\begin{bmatrix} y_1 \\ y_2 \\ y_3 \end{bmatrix} | \mathbf{x}^b, c\right) \times P([y_4] | \mathbf{x}^b, c)$$

For day-time AATSR retrievals, the 3.7 μm channel is replaced with the 1.6 μm channel, to avoid problems with solar contamination.

<p>The University of Edinburgh</p> 	<p>ATSR Reprocessing for Climate Lake Surface Water Temperature – ARC-Lake</p>	<p>Document Ref: ARC-Lake-ATBD-v1.3 Issue: 1 Date: 23 Oct 2013</p>
--	--	--

6.2.2 Definitions

If it is assumed that the errors in the observed and background brightness temperatures have a Gaussian distribution, then the joint probability density function is given by:

$$\text{Eq. 6.3} \quad P(\mathbf{y}_s^o | \mathbf{x}^b, c) = \frac{\exp \left\{ -\frac{1}{2} \Delta \mathbf{y}^T (\mathbf{K} \mathbf{S}_a \mathbf{K}^T + \mathbf{S}_\varepsilon)^{-1} \Delta \mathbf{y} \right\}}{2\pi |\mathbf{K} \mathbf{S}_a \mathbf{K}^T + \mathbf{S}_\varepsilon|^{1/2}}$$

which for the AATSR example can be written as:

$$\text{Eq. 6.4} \quad P \left(\begin{bmatrix} y_1 \\ y_2 \\ y_3 \end{bmatrix} | \mathbf{x}^b, c \right) = \frac{\exp \left\{ -\frac{1}{2} \Delta \mathbf{y}^T (\mathbf{K} \mathbf{S}_a \mathbf{K}^T + \mathbf{S}_\varepsilon)^{-1} \Delta \mathbf{y} \right\}}{2\pi |\mathbf{K} \mathbf{S}_a \mathbf{K}^T + \mathbf{S}_\varepsilon|^{1/2}}$$

If the clear-sky probability density evaluates to less than 10^{-15} K^{-2} , it is set to 10^{-15} K^{-2} . In conjunction with a minimum of 10^{-10} K^{-2} imposed on the cloudy probability density function, this means that any outlying/aberrant BTs are flagged as not clear, while avoiding dividing by zero.

The vector and matrix terms in Eq. 6.3 are defined as follows:


- (i) $\Delta \mathbf{y}$ is the difference vector for the observed and background brightness temperatures, defined for the i th element as $y_i^b = F_i(\mathbf{x}^b)$.
 - (ii) $\mathbf{K} \mathbf{S}_a \mathbf{K}^T$ is the error covariance in the background observation vector resulting from the propagation of the background variable errors through the FFM.
- \mathbf{K} is the tangent linear of the forward model defined as:

$$\mathbf{K} = \frac{\partial \mathbf{y}_s^b}{\partial \mathbf{x}^b}$$

For the example of AATSR, \mathbf{K} can be written as:

$$\mathbf{K} = \begin{bmatrix} \frac{\partial T_{3.9}}{\partial SST^b} & \frac{\partial T_{3.9}}{\partial TCWV^b} \\ \frac{\partial T_{11}}{\partial SST^b} & \frac{\partial T_{11}}{\partial TCWV^b} \\ \frac{\partial T_{12}}{\partial SST^b} & \frac{\partial T_{12}}{\partial TCWV^b} \end{bmatrix}$$

\mathbf{S}_a is the background covariance matrix defined as

<p>The University of Edinburgh</p> 	<p>ATSR Reprocessing for Climate Lake Surface Water Temperature – ARC-Lake</p>	<p>Document Ref: ARC-Lake-ATBD-v1.3 Issue: 1 Date: 23 Oct 2013</p>
--	--	--

$$\mathbf{S}_a = \begin{bmatrix} (\varepsilon_{SST}^b)^2 & 0 \\ 0 & (\varepsilon_{TCWV}^b)^2 \end{bmatrix}$$

where ε_{SST}^b and ε_{TCWV}^b are the errors in the background state variables.

- (iii) \mathbf{S}_ε is the total covariance in the difference between the background and actual observation vectors in the absence of background variable error. This is the sum of the RTM model covariance and the covariance in the observed values. The examples below illustrate the three-channel case (e.g. AATSR night-time retrievals, where $i = 3.7 \mu\text{m}$, $j = 11 \mu\text{m}$, and $k = 12 \mu\text{m}$), and are readily generalized to other configurations.

$$\mathbf{S}_r = \begin{bmatrix} (\varepsilon_i^m)^2 & r^2(\varepsilon_i^m)(\varepsilon_j^m) & r^2(\varepsilon_i^m)(\varepsilon_k^m) \\ r^2(\varepsilon_j^m)(\varepsilon_i^m) & (\varepsilon_j^m)^2 & r^2(\varepsilon_j^m)(\varepsilon_k^m) \\ r^2(\varepsilon_k^m)(\varepsilon_i^m) & r^2(\varepsilon_k^m)(\varepsilon_j^m) & (\varepsilon_k^m)^2 \end{bmatrix}$$

where r is the correlation coefficient of RTM error between the two channels. By default, the errors in the modelled brightness temperatures are assumed to be uncorrelated, i.e., $r^2 = 0$ (which needs further assessment).

The other variance component for the observed brightness temperatures is due to radiometric noise, which is assumed to be uncorrelated between TIR channels, therefore the covariance matrix for the observed parameters is:

$$\mathbf{S}_o = \begin{bmatrix} (\varepsilon_i^o)^2 & 0 & 0 \\ 0 & (\varepsilon_j^o)^2 & 0 \\ 0 & 0 & (\varepsilon_k^o)^2 \end{bmatrix}$$

The sum of the covariances in the RTM model and observed values gives the total covariance matrix:

$$\text{Eq. 6.5} \quad \mathbf{S}_\varepsilon = \mathbf{S}_r + \mathbf{S}_o = \begin{bmatrix} (\varepsilon_i^m)^2 + (\varepsilon_i^o)^2 & r^2(\varepsilon_i^m)(\varepsilon_j^m) & r^2(\varepsilon_i^m)(\varepsilon_k^m) \\ r^2(\varepsilon_j^m)(\varepsilon_i^m) & (\varepsilon_j^m)^2 + (\varepsilon_j^o)^2 & r^2(\varepsilon_j^m)(\varepsilon_k^m) \\ r^2(\varepsilon_k^m)(\varepsilon_i^m) & r^2(\varepsilon_k^m)(\varepsilon_j^m) & (\varepsilon_k^m)^2 + (\varepsilon_k^o)^2 \end{bmatrix}$$

NOTE: The example for AATSR night-time pixels can be easily modified to perform cloud screening for day-time pixels. For the day-time case, the $3.7 \mu\text{m}$ channel is replaced by the near-infrared channel, giving $i = 1.6 \mu\text{m}$ in Eq. 6.5. Again, $r^2 = 0$ is appropriate, since the forward models are independent.

6.2.3 LSD Distributions

The texture measure used in ARC-Lake is local standard deviation (LSD) and has a non-Gaussian distribution, for both clear and cloudy scenes. A satisfactory analytical solution has not been found, and PDFs for the textural component are derived empirically from pre-screened observations over oceans. Since the spatial distribution of thermal features and gradients in lakes can be different over lakes (typically, less uniformity than the ocean), creation of a PDF specific to inland waters will be considered in future. The distribution of local standard deviation for clear-sky cases also depends on radiometric noise. Lower channel noise requires a higher bin resolution to accurately represent the peak in the PDF. The low-noise (NEDT ~ 0.04 K) 1 km resolution ATSR2/AATSR are used to create the pdfs empirically. A 1-D textural PDF for the 11 μm channel is used for ATSR-2 and AATSR night-time (Figure 2) and day-time retrievals.

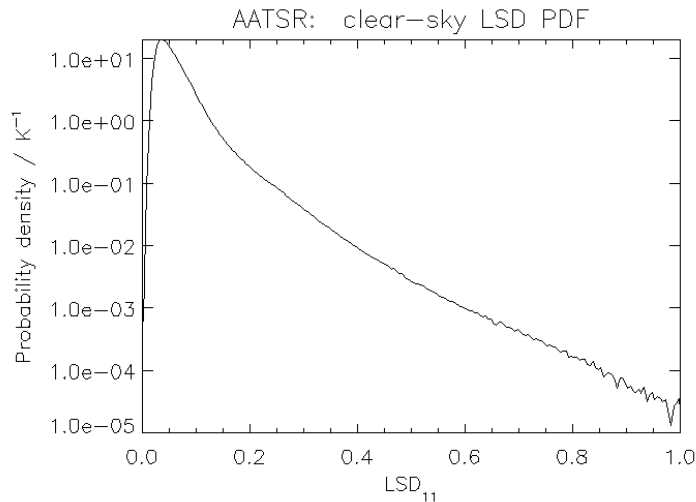


Figure 2. Clear-sky 11 μm textural PDF for night-time AATSR.


6.3 Probability density functions – cloudy-sky

6.3.1 Definitions

$P(y^o | x^b, \bar{c})$ is the probability of the observations given the background fields and assuming cloudy-sky (the condition ‘*not clear-sky*’ is more correct as this condition could also result from extreme aerosol loading or clear-sky over ice). As with the clear-sky probabilities, it will be assumed that the local standard deviation PDFs are independent of the brightness temperatures (and reflectances), therefore for the cloudy probability

$$\text{Eq. 6.6. } P(y^o | x^b, \bar{c}) = P(y_s^o | x^b, \bar{c}) \times P(y_t^o | x^b, \bar{c})$$

For the AATSR example (as introduced in §6.2.1), Eq. 6.6 can be written as:

<p>The University of Edinburgh</p> 	<p>ATSR Reprocessing for Climate Lake Surface Water Temperature – ARC-Lake</p>	<p>Document Ref: ARC-Lake-ATBD-v1.3 Issue: 1 Date: 23 Oct 2013</p>
--	--	--

$$\text{Eq. 6.7 } P(\mathbf{y}^o | \mathbf{x}^b, \bar{c}) = P\left(\begin{bmatrix} y_1 \\ y_2 \\ y_3 \end{bmatrix} | \mathbf{x}^b, \bar{c}\right) \times P(y_4 | \mathbf{x}^b, \bar{c})$$

6.3.2 Joint BT Distributions

The joint probability density function $P(\mathbf{y}^o | \mathbf{x}^b, \bar{c})$ will have no analytic form and must be inferred from empirical observations or numerical modelling and then tabulated.

The approach taken in the ARC-Lake processor is to define $P(\mathbf{y}^o | \mathbf{x}^b, \bar{c})$ as a function of only one variable in the background state, \mathbf{x}^b , namely, the prior surface temperature. The tabulations have been defined within the ARC SST project for cloud radiances associated with different bands of prior SST, and are assumed to apply similarly for different LSWTs.

The global joint probability density function (hereafter, ‘*P-cloud*’), derived empirically from satellite imagery or numerical modelling, is represented by an N -dimensional look-up table (LUT), where N is the number of channels used (and must match the number of channels used to define the clear scene PDF, §6.2). Appropriate bin widths must be chosen so as to give as smooth a representation of the PDF as possible given the number of data points. The PDFs must also be correctly normalized so that their units match the analytical PDF for $P(\mathbf{y}^o | \mathbf{x}^b, c)$. It is also necessary to define a minimum allowed value for elements of all PDFs, with any values less than this reset to the minimum. In ARC-Lake, the LUTs for ‘*P-cloud*’ derived from the ARC SST project is used.

For the AATSR example (§6.2.1), *P-cloud* is taken from cloud-screened ocean imagery of AATSR. The *P-cloud* is defined as the fraction of known cloudy-pixel BTs occurring in each bin of size 2 K along the dimension T_{11} -SST and of size $(0.2 \text{ K})^2$ in the area defined by axes $\{T_{11}-T_{12}, T_{3.7}-T_{11}\}$. The occurrences counted are those flagged cloudy in the ARC SST mask from all AATSR night-time images from all latitudes and seasons, giving a huge number of observations from which to deduce a smooth LUT. *P-cloud* was determined for nadir and forward views separately and as a function of prior SST. As a method of compression, the *P-cloud* LUTs are stored in terms of temperature differences (e.g, 3.7 μm - 11 μm , 11 μm - 12 μm , and 11 μm – SST for the AATSR night-time example).

Slices of the *P-cloud* LUT for the AATSR example are shown in Figure 3 for the nadir view and a prior SST or LSWT of 280.0-282.5 K. The full night-time LUT is an array of dimensions [2,14,80,50,15] corresponding to dimensions of: satellite zenith angle, prior SST, 3.7 μm - 11 μm , 11 μm - 12 μm , and 11 μm – SST. Bin sizes for these dimensions are: 30°, 2.5 K, 0.2 K, 0.2 K, and 2 K. Ranges vary for dimensions representing temperature differences, while the SST dimension covers from 270.0 K to 305.0 K. The minimum is not zero, but is set to 10^{-10} K^2 . This is to avoid geophysically implausible values of BT being given zero probability of there being cloud: the minimum of the clear-sky probability density

function is set to 10^{-15} K^2 , and so BT outliers will be flagged as ‘*not clear*’, as one would wish.

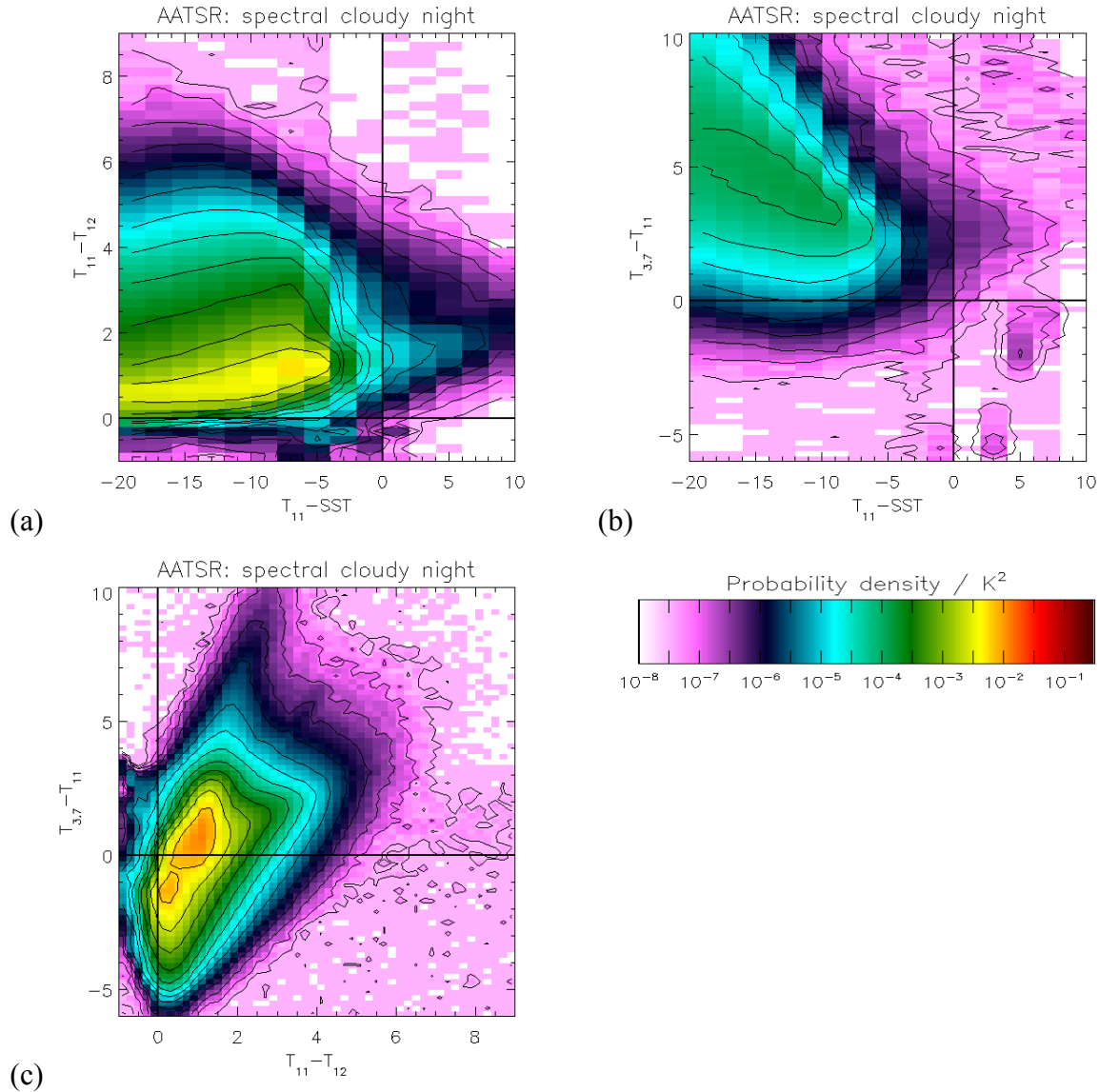



Figure 3. Examples of slices of the night-time cloudy-sky spectral PDF LUT for AATSR. All figures illustrate the LUT used for the nadir view for a prior LSWT range of 280.0 K to 282.5 K. (a) $11 \mu\text{m} - \text{SST}$ vs $11 \mu\text{m} - 12 \mu\text{m}$ for $3.7 \mu\text{m} - 11 \mu\text{m}$ differences of 2.0 K to 2.2 K. (b) $11 \mu\text{m} - \text{SST}$ vs $3.7 \mu\text{m} - 11 \mu\text{m}$ for $11 \mu\text{m} - 12 \mu\text{m}$ differences of 4.0 K to 4.2 K. (c) $11 \mu\text{m} - 12 \mu\text{m}$ vs $3.7 \mu\text{m} - 11 \mu\text{m}$ for $11 \mu\text{m} - \text{SST}$ differences of -6.0 K to -4.0 K.

For the day-time AATSR example, $P\text{-cloud}$ is determined for the dual-view configuration rather than for each view separately as in the night-time case. This dual-view method is only possible for day-time retrievals as the reduced TIR channel set enables a manageable-sized LUT to be defined. As for night-time retrievals, $P\text{-cloud}$ is determined as a function of prior SST and the LUTs are stored in terms of temperature differences. The full day-time LUT is

<p>The University of Edinburgh</p> 	<p>ATSR Reprocessing for Climate Lake Surface Water Temperature – ARC-Lake</p>	<p>Document Ref: ARC-Lake-ATBD-v1.3 Issue: 1 Date: 23 Oct 2013</p>
--	--	--

an array of dimensions [14, 15, 20, 20, 20] corresponding to: prior SST, 11 μ m nadir – SST, 11 μ m nadir - 12 μ m nadir, 11 μ m forward - 12 μ m forward, 11 μ m nadir – 11 μ m forward. Bin sizes for these dimensions are: 2.5 K, 2.0 K, 0.4 K, 0.4 K, and 0.4 K. *P-cloud* for the AATSR day –time example is shown in Figure 4 for a prior SST of 280.0 K to 282.5 K.

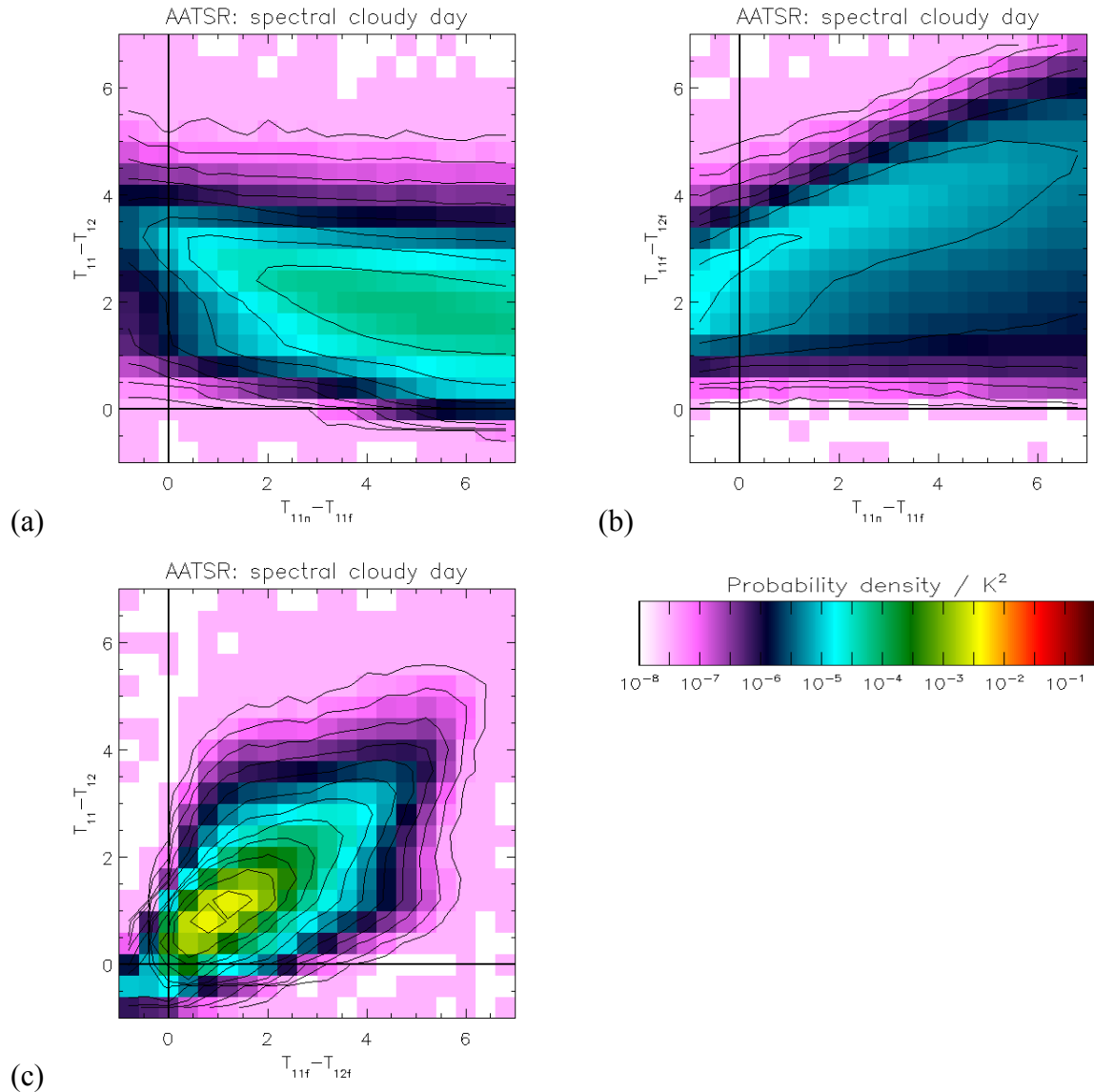



Figure 4. Examples of slices of the day-time cloudy-sky spectral PDF LUT for AATSR. All figures are illustrative for a prior SST range of 280.0 K to 282.5 K and 11 μ m – SST differences of -6.0 K to -4.0 K. (a) 11 μ m nadir – 11 μ m forward vs 11 μ m nadir – 12 μ m nadir for 11 μ m forward – 12 μ m forward differences of 3.0 K to 3.4 K. (b) 11 μ m nadir – 11 μ m forward vs 11 μ m forward – 12 μ m forward for 11 μ m nadir – 12 μ m nadir differences of 3.0 K to 3.4 K. (c) 11 μ m forward – 12 μ m forward vs 11 μ m nadir – 12 μ m nadir for 11 μ m nadir – 11 μ m forward differences of 3.0 K to 3.4 K.

<p>The University of Edinburgh</p> 	<p>ATSR Reprocessing for Climate Lake Surface Water Temperature – ARC-Lake</p>	<p>Document Ref: ARC-Lake-ATBD-v1.3 Issue: 1 Date: 23 Oct 2013</p>
--	--	--

It is assumed that the near infra-red (NIR) reflectance ($1.6 \mu\text{m}$) is uncorrelated with the TIR BTs ($11 \mu\text{m}$ and $12 \mu\text{m}$ for AATSR), therefore for the day-time pixels the general form of the globally cloudy PDF is given by:

$$\text{Eq. 6.8} \quad P(\mathbf{y}_s^o | \bar{c}) = P(y_{NIR} | \bar{c}) \times P(y_{TIR} | \bar{c})$$

For the AATSR example this is:

$$\text{Eq. 6.9} \quad P\left(\begin{bmatrix} y_{NIR} \\ y_2 \\ y_3 \end{bmatrix} | \bar{c}\right) = P(y_{NIR} | \bar{c}) \times P\left(\begin{bmatrix} y_2 \\ y_3 \end{bmatrix} | \bar{c}\right)$$

where $P\text{-cloud}$ for the NIR reflectance is determined for the dual-view configuration in a similar manner to that outlined above. The full day-time LUT for the NIR reflectance is an array of dimensions $[28, 100, 100]$ corresponding to: solar zenith angle, $1.6 \mu\text{m}$ nadir, and $-1.6 \mu\text{m}$ forward. Bin sizes for these dimensions are: 2.5° , 0.01 , and 0.01 . $P\text{-cloud}$ for the AATSR day-time reflectance channel is shown in Figure 5 for a solar zenith angle range of 55° to 57.5° .

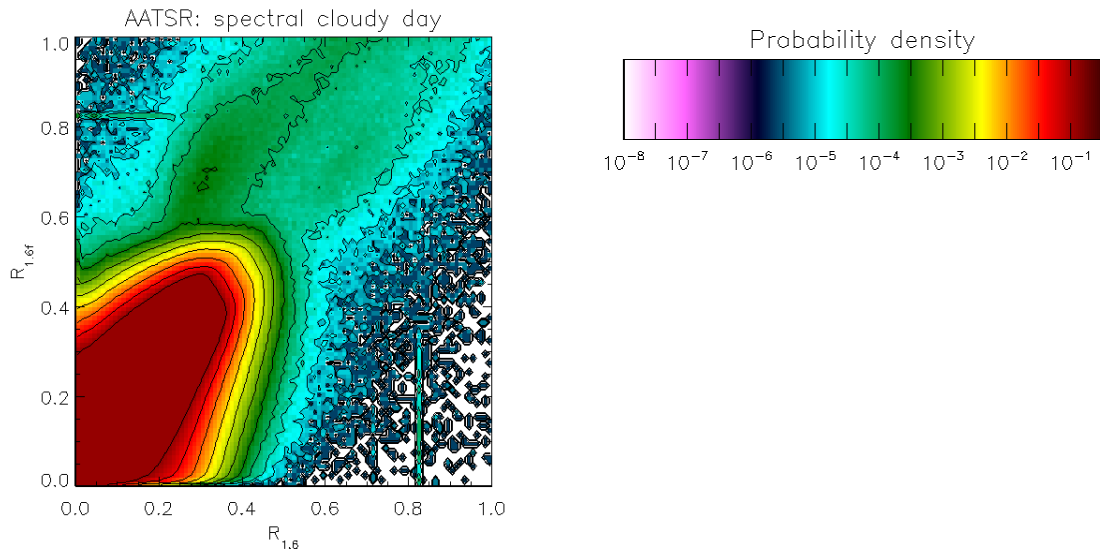


Figure 5. Example slice of cloudy-sky spectral PDF LUT for $1.6 \mu\text{m}$ day-time for solar zenith angles in the range 55° to 57.5° .

6.3.3 LSD Distributions

The joint probability distribution $P(\mathbf{y}_t^o | \mathbf{x}^b, \bar{c})$ of LSD for TIR channels can be determined empirically from pre-screened observations (the cloudy scene is too complex to be represented analytically). Textural measures are only useful for screening over water surfaces where the length of scale of variability can be assumed to be much larger than the pixel scale. For SST retrievals this is generally true, except in regions of ocean fronts. For LSWT

retrievals however, the length of scale of variability may be shorter and this assumption may no longer be adequate. Therefore further assessment of LSD distributions for lakes is required.

For the AATSR example, $P(y_i^o | x^b, \bar{c})$ of LSD for 11 μm was found empirically from cloudy pixels in the full set of AATSR imagery. The probability function estimated is shown in Figure 6.

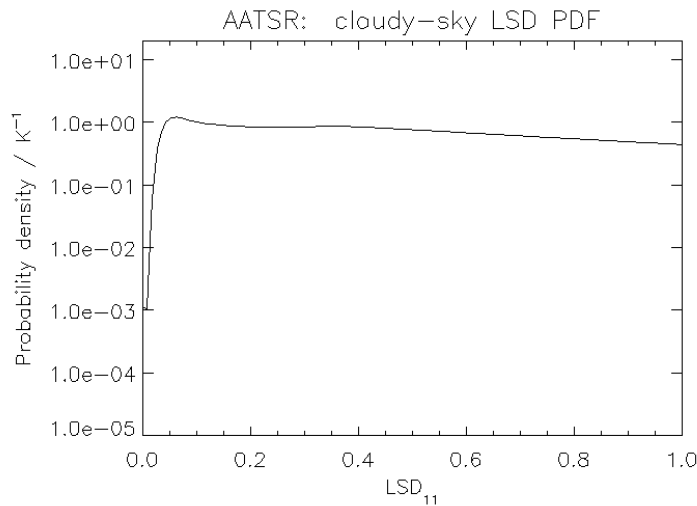


Figure 6. Cloudy-sky 11 μm textural PDF for night-time AATSR.

6.4 Clear-sky Probability

6.4.1 Unconditional clear-sky probability - $P(c)$


The unconditional clear-sky probability is currently set to a globally constant value of 10%, i.e.

Eq. 6.10 $P(c) = 0.10$

Using an existing database of imagery for a given satellite sensor this PDF could be improved to allow for the spatial and seasonal variability in clear-sky conditions. From a longer time series it will also be possible to allow for climatic patterns such as the El Nino southern oscillation (ENSO) and the North Atlantic oscillation (NAO) which both significantly affect cloud distributions. However, the influence of this parameter is not dominant, and these refinements are not a priority.

6.4.2 Conditional clear-sky probability - $P(c | y^o, x^b)$

The conditional clear-sky probability is a measure of the likelihood of a given pixel being cloud-free, and is the value returned as part of the SST product. It is calculated using the equation:

<p>The University of Edinburgh</p> 	<p>ATSR Reprocessing for Climate Lake Surface Water Temperature – ARC-Lake</p>	<p>Document Ref: ARC-Lake-ATBD-v1.3 Issue: 1 Date: 23 Oct 2013</p>
--	--	--

$$\text{Eq. 6.11} \quad P(c | y^o, x^b) = \left[1 + \frac{P(\bar{c})P(y^o | x^b, \bar{c})}{P(c)P(y^o | x^b, c)} \right]^{-1}$$


where $P(\bar{c}) = 1 - P(c)$

$P(y^o | x^b, c)$ is defined in §6.2

$P(y^o | x^b, \bar{c})$ is defined in §6.3

6.5 Practical considerations

The LUTs for all PDFs are stored across two files per instrument: one for clear-sky probabilities and the other for cloudy-sky probabilities. These files are in NetCDF format. Each file contains the various LUTs along with data defining the dimensions of each LUT. Selection of LUTs from these files and the look-up of the LUTs is handled by the ARC-Lake processing code, and is dependent on the following factors: channels available, solar zenith angle, satellite zenith angle, prior LSWT, and the channel BTs and reflectances.

<p>The University of Edinburgh</p> 	<p>ATSR Reprocessing for Climate Lake Surface Water Temperature – ARC-Lake</p>	<p>Document Ref: ARC-Lake-ATBD-v1.3 Issue: 1 Date: 23 Oct 2013</p>
--	--	--

7 ICE IN PIXEL TEST

The ARC-Lake project also provides observations of lake ice concentration (LIC). This is based on the Normalized Difference Snow Index (NDSI) of Hall et al (1995) and is limited to daytime observations (as it uses visible reflectance channels). The NDSI is calculated using

$$\text{Eq. 7.1} \quad NDSI = \frac{R_{0.8} - R_{1.6}}{R_{0.8} + R_{1.6}}$$

Where $R_{0.8}$ and $R_{1.6}$ are the reflectance observations in the 0.87 μm and 1.6 μm channels respectively. Image pixels where $NDSI > 0.5$ are flagged as ice.


The NDSI test is only performed on pixels that pass a prior threshold test, based on reflectances in the 0.67 μm , 0.87 μm and 1.6 μm channels:

$$2 \times R_{0.8} - R_{0.6} - R_{1.6} > 0.003$$


This threshold test is included to prevent excessive flagging of open-water pixels as ice, and is derived empirically from AATSR imagery over oceans. In some cases this test results in ice pixels being flagged as open-water (MacCallum and Merchant, 2011b) and therefore an underestimation of ice cover in some scenes.

Coarse cloud screening, performed in advance of this ice test in the retrieval scheme, results in some ice pixels being flagged as cloud rather than ice, if the ice is very cold (around -10°C or colder, depending on the atmospheric conditions). This resulted in an underestimation of ice cover in some scenes in v1.0. To reduce the impact of this effect, the ice test is performed in advance of the coarse cloud screening in v1.1 onwards. The ice test is also prone to occasional false positive flagging ice-clouds as surface ice, with some cloud pixels being flagged as ice. In v1.1 onwards the impact of this effect is again reduced, through an additional threshold test: observations are only flagged as ice for cases where the prior LSWT < 278 K. For ATSR-2 there may also be occasional times when this ice test cannot be performed due to erroneous or unpredictable switching from the 1.6 μm to 3.7 μm channel (Mutlow *et al*, 1999). This can happen when reflectances are particularly low (e.g. when the surface is in shadow). The more general effect of shading on reflectances and any subsequent impact on NDSI is a relevant issue for lakes, due to potential shading effects of topography and cloud cover. (For ATSR-1, there is no 0.87 μm channel, and LIC is not generated.)

The LIC field in the ARC-Lake products then reports the fraction of clear-sky (i.e., not flagged as cloudy) lake pixels in the cell in which surface ice was flagged as above.

<p>The University of Edinburgh</p> 	<p>ATSR Reprocessing for Climate Lake Surface Water Temperature – ARC-Lake</p>	<p>Document Ref: ARC-Lake-ATBD-v1.3 Issue: 1 Date: 23 Oct 2013</p>
---	---	--

The limitations are thus suspected low hit rate for surface ice (when classed as cloud instead) and suspected significant false alarm rate (when ice cloud is classed as surface ice). These statements cannot be quantified at time of writing. Future work should involve assessing the (mis)classification rate, synthesizing feedback from users regarding the LIC product, reviewing the literature for improvements/additions to the scheme and devising or implementing such improvements.

<p>The University of Edinburgh</p> 	<p>ATSR Reprocessing for Climate Lake Surface Water Temperature – ARC-Lake</p>	<p>Document Ref: ARC-Lake-ATBD-v1.3 Issue: 1 Date: 23 Oct 2013</p>
--	--	--

8 LAKE SURFACE WATER TEMPERATURE RETRIEVAL WITH UNCERTAINTY

Using standard ATSR SST retrieval coefficients for LSWT retrievals is prone, for some lakes, to retrieval biases of 0.5 K (Marsham, 2003). (By retrieval bias, we mean the systematic offset between satellite and true LSWT that arises from imperfection in the retrieval algorithm. Occasional “biases” from failures in cloud detection can be larger.) This contrasts with a level of SST retrieval bias for ATSR that is generally <0.2 K. The relatively larger potential for bias arises because of the range of lake altitudes, emissivity and the continentality of air masses; all these factors change the relationships between BTs and surface temperature. One solution could be to specify lake-specific retrieval coefficients. But this is not really a scalable solution as we look forward to later phases of the project, where more lakes will be tackled.


The LSWT retrieval is therefore done by optimal estimation (OE). We use a simplified formulation of the inverse problem originally developed for SST observations from the Advanced Very High Resolution Radiometer (AVHRR) (Merchant *et al*, 2008). This formulation includes only LSWT and total column water vapour as retrieved (state) variables (all though full profile forward modelling is of course used). No radiance bias correction is yet derived for ATSR BTs, so the RTTOV8.7-simulated BTs are used “as is”

8.1 Optimal Estimation (OE) Retrievals

Optimal Estimation (OE) techniques combine prior information on the expected state of the atmosphere and the lake surface with observations to provide an optimal solution of the state and an associated uncertainty estimate.

Prior information, referred to as the prior state vector and denoted \mathbf{x}_a , where the “a” subscript denotes *a priori*, consists of: NWP forecast fields, reconstructed lake temperatures derived from ARC-Lake observations (§4), and a modelled estimate of emissivity (§5). This *a priori* information is input into a forward model to simulate observations for the prior state, $\mathbf{y}_a = \mathbf{F}(\mathbf{x}_a)$. The forward model used in ARC-Lake is RTTOV8.7 (Brunel *et al*, 2005), which provides simulated BTs corresponding to the ATSR channels. Partial derivatives of these simulated BTs with respect to state variables are also calculated. These provide an estimate of the sensitivity of the prior observations to the state. This sensitivity information is combined with the differences between satellite observations, \mathbf{y}_o , and prior observations, \mathbf{y}_a , to estimate the actual state.

The process is optimal in the sense that it will give an unbiased, minimum SD estimate provided the prior information, forward model and error covariance estimates are unbiased

<p>The University of Edinburgh</p> 	<p>ATSR Reprocessing for Climate Lake Surface Water Temperature – ARC-Lake</p>	<p>Document Ref: ARC-Lake-ATBD-v1.3 Issue: 1 Date: 23 Oct 2013</p>
--	--	--

(Merchant *et al*, 2008). Two additional assumptions are also made: the retrieval is assumed to be linear within the range of BT corresponding to errors in NWP fields and that only the leading two terms controlling BT need be considered. The second of these assumptions leads to a reduced state vector, $\mathbf{z}(\mathbf{x}) = \begin{bmatrix} x \\ w \end{bmatrix}$, in the retrieval, where x and w are the LSWT and total column water vapour respectively. However, the full prior state vector, \mathbf{x}_a , is used in the forward model.

The optimal solution is a weighted combination of the prior LSWT and TCWV, $\mathbf{z}(\mathbf{x}_a)$, and the difference between the observations, \mathbf{y}_o , and the BTs simulated for the prior field, $\mathbf{y}_a = \mathbf{F}(\mathbf{x}_a)$. Following the methods of Rodgers (1990) and Rodgers (2000), the equation for this solution is:

$$\text{Eq. 8.1} \quad \hat{\mathbf{z}} = \mathbf{z}(\mathbf{x}_a) + (\mathbf{K}^T \mathbf{S}_\varepsilon^{-1} \mathbf{K} + \mathbf{S}_a^{-1})^{-1} \mathbf{K}^T \mathbf{S}_\varepsilon^{-1} (\mathbf{y}_o - \mathbf{F}(\mathbf{x}_a))$$

where $\hat{\mathbf{z}}$ consists of the retrieved LSWT and TCWV, \mathbf{K} is the matrix of partial derivatives of observations with respect to the state, \mathbf{S}_ε is the combined covariance matrix of prior and satellite observations, and \mathbf{S}_a is the prior covariance matrix of the reduced state vector.

For day-time ARC-Lake LSWT retrievals these matrices are defined as follows (in Eq. 8.2 to Eq. 8.4). For night-time retrievals, the retrieval methodology outlined below is expanded to include the 3.7 μm channel.

$$\text{Eq. 8.2} \quad \mathbf{K} = \left[\frac{\partial \mathbf{F}(\mathbf{x}_a)}{\partial \mathbf{z}} \right] = \begin{bmatrix} \partial y_{11} / \partial x & \partial y_{11} / \partial w \\ \partial y_{12} / \partial x & \partial y_{12} / \partial w \end{bmatrix}$$

where y_{11} and y_{12} represent the simulated BTs for the 11 μm and 12 μm channels, for the prior state, \mathbf{x}_a . The tangent linear outputs of the forward model, RTTOV, are used to represent \mathbf{K} .

$$\text{Eq. 8.3} \quad \mathbf{S}_\varepsilon = \begin{bmatrix} e_{11}^2 & 0 \\ 0 & e_{12}^2 \end{bmatrix}$$

where it is assumed that both radiometric noise in the satellite BTs and forward modelling errors are uncorrelated between channels (indicated by zero-value off-diagonal terms). Radiometric noise is calculated as a function on BT, based on channel NEAT values at calibration black-body temperatures.

<p>The University of Edinburgh</p> 	<p>ATSR Reprocessing for Climate Lake Surface Water Temperature – ARC-Lake</p>	<p>Document Ref: ARC-Lake-ATBD-v1.3 Issue: 1 Date: 23 Oct 2013</p>
--	--	--

Eq. 8.4

$$\mathbf{S}_a = \begin{bmatrix} e_{x_a}^2 & 0 \\ 0 & e_{w_a}^2 \end{bmatrix}$$

where the zero-value off-diagonal terms indicate that errors in the prior LSWT and TCWV are assumed to be independent. The prior uncertainty in LSWT is determined from comparisons of retrieved LSWT with *in situ* observations (§4), while the prior uncertainty in TCWV is calculated as a function of TCWV, using coefficients derived from analysis on the ARC SST match-up database.

The expected total random uncertainty in \hat{z} is represented by the error covariance matrix:

Eq. 8.5

$$\hat{\mathbf{S}} = (\mathbf{K}^T \mathbf{S}_e^{-1} \mathbf{K} + \mathbf{S}_a^{-1})^{-1}$$

which includes the effects of instrumental noise, random forward model error, and errors in the prior state. Here, the leading element of $\hat{\mathbf{S}}$ provides an estimate of the random Gaussian variance in the retrieved LSWT from the sources above. Full details of the treatment of uncertainties in the LSWT retrieval is given in §8.2.

8.2 Treatment of Uncertainties

8.2.1 Introduction

All LSWT retrievals have an associated uncertainty estimate. Appropriate consideration and incorporation of uncertainties from all possible sources is important for any LSWT retrieval scheme. Uncertainties are typically split into two broad categories: systematic and random. Systematic uncertainties are described in terms of bias and give a measure of the accuracy of the retrieval. This is normally estimated by the mean difference between retrieved values and “truth” data (e.g. *in situ* buoy measurements). Random uncertainties are described in terms of scatter and provide an estimate of the precision of the retrieval. The standard deviation (SD) of the differences between retrieved and “truth” data are commonly used to estimate (or give an upper bound on) this uncertainty. Although these basic categorisations may be used to provide an overall picture of the errors in a retrieval scheme, error characteristics are in reality more complex, as discussed below.

It should be noted that in ARC-Lake v2.0 products, the uncertainty estimate provided, “Err_LSWT” (MacCallum and Merchant, 2011a), is simply an estimate of the variance of LSWT observations within each 0.05°x0.05° grid cell. The treatment of errors as discussed in the following sections will be implemented in later versions of ARC-Lake products.

8.2.2 Systematic Errors

General comment

Uncertainty distributions for systematic errors are not included in the uncertainty estimates associated with LSWTs in the ARC-Lake products. The reason is that systematic errors

<p>The University of Edinburgh</p> 	<p>ATSR Reprocessing for Climate Lake Surface Water Temperature – ARC-Lake</p>	<p>Document Ref: ARC-Lake-ATBD-v1.3 Issue: 1 Date: 23 Oct 2013</p>
--	--	--

(biases) are subject to characterisation and reduction by, for example, improved retrieval algorithms. Information about biases is given by validation against independent measurements. The sections below, however, discuss some forms of systematic errors relevant to ARC-Lake, for information.

Forward modelling errors

Systematic errors are introduced to the retrieval through the forward model, specified in §8.1, that is used to simulate radiances, \mathbf{y} , where:

$$\text{Eq. 8.6} \quad \mathbf{y} = \mathbf{F}(\mathbf{x}, \mathbf{b}) + \varepsilon_F$$

Here, \mathbf{F} represents the function of the RTM, and ε_F the radiative transfer model error. The surface and atmospheric state are described by \mathbf{x} , while \mathbf{b} incorporates other model parameters such as spectroscopic data and sensor characterisation. The RTM error, ε_F , represents the departure of the simulation from what would really be observed by a sensor observing the situation described by \mathbf{x} and \mathbf{b} , but it does not account for errors due to systematic differences between state vectors and reality or errors in the model parameters. Including these errors, the full forward model error can be described as:

$$\text{Eq. 8.7} \quad \varepsilon_y = \varepsilon_F + \frac{\partial F}{\partial \mathbf{x}} \varepsilon_x + \frac{\partial F}{\partial \mathbf{b}} \varepsilon_b$$

where the subscripts of ε define the parameter in error. As discussed by Merchant and Le Borgne (2004), any or all of the terms in Eq. 8.7 can be significant in the context of SST (and therefore LSWT) retrievals.

The forward model error, ε_y , propagates through into the LSWT retrieval error. Contributions to the error from forward model parameters can be isolated by performing identical radiative transfer simulations, except for perturbed values of the parameters of interest. Defining \mathbf{y}_p as the BTs simulated after a perturbation, Δb , of parameter, b , of the forward model, the resulting error in BT from a parameter error of size Δb can be defined as:

$$\text{Eq. 8.8} \quad \mathbf{e}_b = \mathbf{y}_a - \mathbf{y}_p \cong \frac{\partial F}{\partial b} \Delta b$$

The associated error in LSWT can be determined from the forward model parameter error covariance matrix, defined by Rodgers (2000) as:

$$\text{Eq. 8.9} \quad \mathbf{S}_f = \mathbf{G}_y \mathbf{K}_b \mathbf{S}_b \mathbf{K}_b^T \mathbf{G}_y^T$$

<p>The University of Edinburgh</p> 	<p>ATSR Reprocessing for Climate Lake Surface Water Temperature – ARC-Lake</p>	<p>Document Ref: ARC-Lake-ATBD-v1.3 Issue: 1 Date: 23 Oct 2013</p>
--	--	--

where $\mathbf{G}_y = (\mathbf{K}^T \mathbf{S}_\varepsilon^{-1} \mathbf{K} + \mathbf{S}_a^{-1})^{-1} \mathbf{K}^T \mathbf{S}_\varepsilon^{-1}$, is the sensitivity of the retrieval to measurement,

$\mathbf{K}_b = \frac{\partial \mathbf{F}}{\partial \mathbf{b}}$, is the sensitivity of the forward model to the forward model parameters, and

$\mathbf{S}_b = \left\langle (\mathbf{b} - \hat{\mathbf{b}})(\mathbf{b} - \hat{\mathbf{b}})^T \right\rangle$, is the error covariance matrix of \mathbf{b} .

The model parameters for which error propagation should be evaluated and an example of their impact on ATSR-2 coefficient-based SST retrievals are given in Table 4.

Model Parameter	Example Perturbation	Δ SST retrieval	
		Bias (K)	Δ SD (%)
Sea surface emissivity	Increase by 0.001 (approximate uncertainty estimate for emissivity)	-0.05	0.4
Trace gas profiles	Change in concentrations from 1999 to 1991 levels.	-0.03	0.03
Water vapour continuum parameterization	Different parameterizations, e.g. CKD 2.2.2 and MT_CKD (see http://www.rtweb.aer.com/), as appropriate at time of implementation	0.01	0.08
Humidity profile	Reduce upper-tropospheric humidity by 15% (systematic error in UTH of this magnitude in NWP profiles is conceivable)	-0.04	6.8
Instrument SRF	Random changes of to the normalized SRF within the SRF uncertainty	-0.12	4.4

Table 4. Model parameters (and example perturbations) for which Eq. 8.9 should be evaluated. Example perturbations and resulting errors are taken from Merchant and Le Borgne (2004) for SST retrievals.

Other systematic errors

There is also a contribution to the overall systematic error from the satellite calibration. The contribution from satellite calibration errors must be assessed by propagating calibration uncertainties through the OE retrieval scheme.

Additional errors caused by stratospheric volcanic aerosol may also need to be considered for the case of ATSR1. Such errors can be considered as systematic, asymmetric errors.

Stratospheric volcanic aerosols have life-times longer than synoptic time scales and affect regions on up to hemispheric space scales.

8.2.3 Random Errors (Uncertainty Estimate) Symmetric (Gaussian) uncertainties

<p>The University of Edinburgh</p> 	<p>ATSR Reprocessing for Climate Lake Surface Water Temperature – ARC-Lake</p>	<p>Document Ref: ARC-Lake-ATBD-v1.3 Issue: 1 Date: 23 Oct 2013</p>
--	--	--

The total uncertainty (Eq 8.5) represents the distribution of three components of error, all of which are assumed to be symmetric and Gaussian. These are: instrumental noise, forward model “noise” and prior error. This is an accurate description of error propagation for a single pixel. However, different components within that total uncertainty differ in their degree of correlation between nearby pixels, and therefore differ in how they should be combined when forming cell-average LSWT. Briefly, the radiometric component is uncorrelated, and the uncertainty reduces with “ $1/\sqrt{n}$ ”, whereas the other components are highly correlated, and the best approximation is to assume no average with respect to the number of pixels within the cell. These comments are expanded below.

Radiometric (instrumental) noise

The radiometric noise in the sensors depends on the scene radiance (or BT) and the temperature of the detector. Radiometric noise expressed as a noise equivalent differential temperature is available to the LSWT retrieval within the processing chain.

The radiometric noise propagates through the LSWT retrieval via the covariance matrix, S_ε , defined in Eq. 6.5, where the contribution from radiometric noise is denoted, S_o . An overall estimate of the radiometric noise in the retrieval can be obtained using

$$\text{Eq. 8.10a} \quad S_m = (K^T S_\varepsilon^{-1} K + S_a^{-1})^{-1} K^T S_o^{-1} K (K^T S_\varepsilon^{-1} K + S_a^{-1})^{-1}$$

The radiometric uncertainty in LSWT, ε_{rad} , is then the square root of the error variance for LSWT, which is the leading term of S_m


Pseudo-random uncertainty

The forward model may have systematic errors, as discussed earlier, but even after correction of these, a distribution of forward modelling errors would remain. We treat these as random to reflect our ignorance, although, of course, for a given NWP profile, the forward model error is (on a given computer) fixed (although unknown). This means that the forward model component of error is highly correlated between nearby pixels in an image, since the same simulations on the NWP profiles have been interpolated to the pixel. In this sense, the forward model uncertainty is pseudo-random rather than truly random.

In addition the prior error is also highly correlated for nearby pixels within a cell, again because the prior information is defined either at tie points or for 0.05° cells – i.e., varies slowly between adjacent pixels.

Thus, the total “pseudo-random” uncertainty is defined by the error covariance matrix:

$$\text{Eq. 8.10b} \quad S_{PR-sym} = (K^T S_\varepsilon^{-1} K + S_a^{-1})^{-1} (K^T S_r^{-1} K + S_a^{-1}) (K^T S_\varepsilon^{-1} K + S_a^{-1})^{-1}$$

<p>The University of Edinburgh</p> 	<p>ATSR Reprocessing for Climate Lake Surface Water Temperature – ARC-Lake</p>	<p>Document Ref: ARC-Lake-ATBD-v1.3 Issue: 1 Date: 23 Oct 2013</p>
--	--	--

The pseudo-random uncertainty in LSWT, ε_{PR-sym} , is then the square root of the error variance for LSWT, which is the leading term of S_{PR-sym} .

Pseudo-random – asymmetric

Another source of pseudo-random error in the LSWT retrievals takes the form of cloud (and perhaps aerosol) contamination in the channel brightness temperatures. This contamination may be a result of either residual cloud in view or reflections from clouds (in the along-track view). The contribution to the overall retrieval error from this source may be determined empirically through comparisons of retrieved LSWTs ($LSWT_{ret}$) with in-situ observations ($LSWT_{buoy}$) for different levels of cloud cover in neighbouring pixels. Comparison of the root-mean-square deviation (RMSD) of the LSWT difference ($\Delta LSWT = LSWT_{ret} - LSWT_{buoy}$), between clear-sky conditions and cases with differing numbers of adjacent cloudy pixels, yields an estimate of the error contribution as a function of cloud cover in adjacent pixels. The asymmetric component of the pseudo-random uncertainty is termed,

$$\varepsilon_{PR-asym}$$

The form of the contribution is cloud-detection and retrieval dependent, and can only be obtained empirically using validation matches. This form of uncertainty is likely to be modified when cloud detection and/or retrieval algorithm are changed. Thus, although it has been assessed for AATSR SST, use of SST-based parameters is therefore not ideal, and this should be re-appraised for lakes using the OE retrieval scheme. A practical difficulty will be that there are greatly fewer matches to validation data for lakes than for SSTs.

Please note, for the reasons above this source of error is described for information purposes only and is **not** accounted for in ARC-Lake v2.0 products. It is not presently clear how and when this uncertainty component will be included.

Thus, for ARC-Lake v2.0, the assumption is “perfect cloud detection”, and $\varepsilon_{PR-asym} = 0$.

Combining random errors

Ideally, the (pseudo) random errors discussed in §8.2.3 are combined to provide an overall estimate of the retrieval error using (treating the asymmetric error as if it were zero mean, which is a conservative assumption):

$$\text{Eq. 8.11} \quad \varepsilon_{total-random} = \sqrt{\varepsilon_{rad}^2 + \varepsilon_{PR-sym}^2 + \varepsilon_{PR-asym}^2}$$

<p>The University of Edinburgh</p> 	<p>ATSR Reprocessing for Climate Lake Surface Water Temperature – ARC-Lake</p>	<p>Document Ref: ARC-Lake-ATBD-v1.3 Issue: 1 Date: 23 Oct 2013</p>
--	--	--

This is the pixel level uncertainty estimate associated with LSWT for each pixel at full resolution. It is consistent with Eq 8.5. The propagation of pixel level uncertainty into the uncertainty associated with a cell average is described in Section 9.

In the ARC-Lake v2.0 products, these errors are not accounted for in the returned error estimate. Radiometric noise and the symmetric component of the pseudo-random uncertainty (ε_{rad} and ε_{PR-sym}) will be introduced by ARC-Lake v3.0.

8.2.4 Other Errors

Other sources of error could also be considered. Incorrect cloud screening (as opposed to undetectable residual cloud contamination characterized as pseudo-random asymmetric error) is one example of such errors. Such errors are occasional and erratic, and cannot be naturally included in the uncertainty estimates. The limitations of the cloud screening method used and the potential errors therefore should be appreciated by users, who can implement quality control or other measures appropriate to their application. Sampling errors may arise from valid clear-sky scenes being flagged as cloudy. This is more likely to eliminate cold than warm features in LSWT. In doing so, warm sampling biases may be introduced into averaged LSWT products.


Another source of sampling error arises from the nature of the ERS/Envisat orbit and swath. As a sun-synchronous polar orbiting satellite, observations are made at a fixed local time on each overpass. Consequently diurnal variations in LSWT cannot be fully captured and diurnal variations in cloud cover may result in consistently low LSWT coverage for some regions. However, this class of “errors” is of a different type to the error estimated with Eq. 8.11, which is an appropriate uncertainty estimate for the LSWT taken for what it is: an observation of LSWT at a particular location and instant.

Sampling errors within areas must be considered when creating and analysing spatially and temporally averaged LSWT products, as in the following section 9.


8.2.5 Confidence Indicators

In addition to the uncertainty information described in §8.2 a further diagnostic on the retrieval is provided in the form of the χ^2 statistic. This provides quantitative measure of the consistency of the retrieval with the satellite observations. The forward model is evaluated for the retrieved state ($\hat{\mathbf{z}} = \begin{bmatrix} \hat{x} \\ \hat{\omega} \end{bmatrix}$) and these simulated BTs compared with the satellite BTs for consistency. The expression used to quantify this is given by Rodgers (2000) as:

$$\text{Eq. 8.12} \quad \hat{\chi}^2 = (\mathbf{K}\hat{\mathbf{z}}' - \mathbf{y}')^T (\mathbf{S}_\varepsilon (\mathbf{K}\mathbf{S}_a \mathbf{K}^T + \mathbf{S}_\varepsilon)^{-1} \mathbf{S}_\varepsilon)^{-1} (\mathbf{K}\hat{\mathbf{z}}' - \mathbf{y}')$$

<p>The University of Edinburgh</p> 	<p>ATSR Reprocessing for Climate Lake Surface Water Temperature – ARC-Lake</p>	<p>Document Ref: ARC-Lake-ATBD-v1.3 Issue: 1 Date: 23 Oct 2013</p>
--	--	--

where $\mathbf{y}' = \mathbf{y} - \mathbf{F}(\mathbf{x}_a)$ and $\hat{\mathbf{z}}' = \hat{\mathbf{z}} - \mathbf{z}_a$. Eq. 8.12 returns a single number as a statistic for each pixel. Provided the OE retrieval is unbiased and errors in the priors and observations are Gaussian and correctly represented in the covariance matrices, the distribution of $\hat{\chi}^2$ should be a $\hat{\chi}^2$ distribution with n degrees of freedom (where n corresponds to the number of channels used in the retrieval). A demonstration of the practical usefulness of the $\hat{\chi}^2$ statistic for a twin-channel retrieval is given by Merchant *et al* (2008). Thus, the $\hat{\chi}^2$ statistic could be interpreted by users as a basis for a confidence indicator akin to the concept used in the SST community (Group for High Resolution SST, GDS 2.0, 2010). At present, the statistic is present, but conversion to a confidence indicator is not provided in ARC-Lake products. If user demand is established for a GHRSSST-style indicator (e.g., in order to convert products to GHRSSST GDS2.0 format), this could be considered in future work.

<p>The University of Edinburgh</p> 	<p>ATSR Reprocessing for Climate Lake Surface Water Temperature – ARC-Lake</p>	<p>Document Ref: ARC-Lake-ATBD-v1.3 Issue: 1 Date: 23 Oct 2013</p>
--	--	--

9 GRIDDING

Spatially and temporally averaged LSWT products are generated for each LSWT retrieval type independently. Averaging is performed using the retrieved LSWT values on the ATSR footprint scale (rather than calculating LSWTs from averaged channel BTs). Only pixels with valid LSWT retrievals for the specific retrieval type are used to produce the averaged LSWT product for that retrieval type, using Eq. 9.1

$$\text{Eq. 9.1} \quad \text{Lake_ST}_{i,j} = \frac{\sum G_{k,l} (\text{Lake_ST}_{k,l})}{\sum G_{k,l}}$$

Here i,j represent the coordinates of the cell in the averaged product, k,l represent the pixel coordinates within the cell of dimension N . $G_{k,l}$ is a cloud-screening operator that takes a value of

0 when the pixel, k,l is cloudy in any of the views used for the current retrieval type

1 when the pixel is cloud-free.

Eq. 9.1 is be used to calculate averaged LSWT products for each retrieval scheme independently. Single-view LSWTs for a given cell may be based on a different sample from any dual-view LSWT for that cell, if the cloud mask for the along-track view differs from the across-track view (which in general it does).

The error estimate associated with $LSWT_{i,j}$ needs to take into account the distinction between random and pseudo-random error, and uncertainty from sub-sampling within the grid cell. It is assumed that radiometric errors are completely uncorrelated between pixels in the cell (true except for cosmetic fill pixels), while PR errors are assumed correlated across the cell (and therefore not reduced by averaging over pixels). The appropriate error estimate is therefore

Eq. 9.2

$$\varepsilon_{i,j} = \sqrt{\frac{\sum G_{k,l} (\varepsilon_{rad,k,l}^2 + \varepsilon_{PR-sym,k,l}^2 + \varepsilon_{PR-asym,k,l}^2)}{(\sum G_{k,l})^2} + \frac{(\sum G_{k,l})}{(\sum G_{k,l})} + \frac{(N - \sum G_{k,l}) \widehat{V}_{Lake_ST,i,j}}{N - 1}}$$


$$\widehat{V}_{Lake_ST,i,j} = \frac{1}{(\sum G_{k,l}) - 1} \sum \left(G_{k,l} x_{k,l} - \frac{\sum (G_{k,l} x_{k,l})}{\sum G_{k,l}} \right); \quad \widehat{V}_{Lake_ST,i,j} \geq V_{min} \text{ if } \sum G_{k,l} < f_{min} N$$

where the first two terms on the right follow directly by analogy with Eq. 9.1 under the assumptions about correlations of errors with the cells. The final term represents the uncertainty in the cell average from sub-sampling, i.e., from the fact that LSWTs under cloud

<p>The University of Edinburgh</p> 	<p>ATSR Reprocessing for Climate Lake Surface Water Temperature – ARC-Lake</p>	<p>Document Ref: ARC-Lake-ATBD-v1.3 Issue: 1 Date: 23 Oct 2013</p>
--	--	--

pixels are not included, and the unknown LSWTs for these pixels are therefore excluded from the cell average. It has the form of an estimate (indicated by the hat symbol) of the true variance of LSWT in the cell, $V_{LSWT,ij}$, scaled by a fraction related to the proportion of the N pixels within the cell boundary that are included in the cell LSWT average. The justification for this model of sampling error is straight-forward: if only one pixel contributes to the cell average LSWT, the uncertainty from this sampling effect is the full variance of LSWT in the cell (as perceived at the ATSR spatial resolution); if all pixels are clear, the sampling uncertainty is zero. The problem is then to find an estimate of $V_{LSWT,ij}$. The options are (i) try to estimate it from the observed data, or (ii) define an external reference (from a climatology of variability at an appropriate resolution for the grid-cells required). Where the grid cell is relatively completely observed, (i) is clearly preferable; however, if relatively few or one pixels are clear within the cell, such an estimate of $V_{LSWT,ij}$ becomes highly uncertain or undefined. The second option is complex to define, being a function of observation resolution, grid cell size, location and seasonality. In the equation above, the option (i) is therefore assumed and the expression for the variance estimate is given. However, for the case where the number of clear pixels is 1 (variance undefined) or less than a fraction f_{min} of the cell (for which the variance estimate is particularly unreliable in the face of spatial correlations within the cell area), a minimum value, V_{min} is imposed $V_{min} = 0.1^2 \text{ K}^2$ and $f_{min} = 0.2$. These parameters are based on judgment (not formally optimized) and are subject to refinement.

As discussed in §8, ARC-Lake v2.0 products provide only an estimate of the variance of LSWT across the cell, and therefore do not implement Eq. 9.2 for the error estimate. Eq. 9.2 will hold for subsequent versions of ARC-Lake products, with $\varepsilon_{PR-asym} = 0$, as discussed in §8.23. It should also be noted that the methods described above to account for uncertainty in the cell average from sub-sampling are not implemented in ARC-Lake v2.0 products, but will again be implemented in subsequent versions.

<p>The University of Edinburgh</p> 	<p>ATSR Reprocessing for Climate Lake Surface Water Temperature – ARC-Lake</p>	<p>Document Ref: ARC-Lake-ATBD-v1.3 Issue: 1 Date: 23 Oct 2013</p>
--	--	--

10 ATSR-1 Modifications


A number of modifications to the processing scheme are implemented for ATSR-1 to account for instrument differences and the effect of aerosols from the Pinatubo eruption in 1991. Some of these have already been described in earlier sections but are summarized here, along with more in depth detail of further ATSR-1 specific modifications.

The lack of visible observing channels results in no ice detection (§7) being performed for ATSR-1. As a consequence, modifications are made to the v2.0 methods used for generating the prior LSWT field (§4.2): ice climatology from ATSR-2/AATSR is substituted into ATSR-1 observations prior to generation of the prior LSWT for the next iteration, and ATSR-2/AATSR climatology is used in preference to FLake simulations and ATSR-1 climatology-based reconstructions.

In addition to modifications already described, two further ATSR-1 specific modifications are implemented: one to correct for variations in the 12 μ m detector temperature and another to account for volcanic aerosol from the Pinatubo eruption in 1991.

Problems with the ATSR-1 cooler resulted in the detector temperature being allowed to rise gradually over the ATSR-1 lifetime. This warming affects all detectors with the 12 μ m channel most significantly affected (Mutlow et al, 1999). The detector warming impacts on the 12 μ m channel in two ways: the radiance to BT conversion is biased due to using the wrong calibration, and the 12 μ m channel response is shifted, modifying the long-wave filter cut-off, and subsequently affecting retrieved LSWTs. The first of these effects is small (<0.01 K) and is corrected for by adjusting the 12 μ m BT using a quadratic fit with dependence on detector temperature. The second of these effects is accounted for through adjustment of the modeled 12 μ m BT. RTTOV 12 μ m BTs are calculated using RTTOV coefficients representing three detector temperatures (85 K, 97.5 K, and 110 K), and the modeled 12 μ m BT for the detector temperature at time of observation derived through linear interpolation of these values.

The eruption of Pinatubo in 1991 resulted in a period of increased aerosol loading in the atmosphere, affecting ATSR-1 BTs. Provided the effects of aerosol are accounted for in the forward model, the performance of the OE retrieval scheme and Bayesian cloud screening are expected to be maintained. Modelled BTs are adjusted by a time, latitude, and satellite zenith angle dependent factor determined from line-by-line model simulations and SST observations from the ARC project over the ATSR-1 lifetime. A latitude and time dependent look-up-table of aerosol index (a measure of the aerosol loading) is estimated from the difference between aerosol robust dual-view and nadir-view SST retrievals. A satellite zenith angle dependent look-up-table of aerosol mode (the change in BT due to the aerosol) is estimated from line-by-line simulations RFM (<http://www.atm.ox.ac.uk/RFM/>) / DISORT (Stamnes et al, 1988) and is combined with the time/latitude varying look-up-table for aerosol index to provide an adjustment factor for the RTTOV modeled BTs.

<p>The University of Edinburgh</p> 	<p>ATSR Reprocessing for Climate Lake Surface Water Temperature – ARC-Lake</p>	<p>Document Ref: ARC-Lake-ATBD-v1.3 Issue: 1 Date: 23 Oct 2013</p>
--	--	--

11 Other Sources of Information

This document describes the theoretical basis for the practical implementation of the ARC-Lake processor for generating Lake Surface Water Temperature (LSWT) and Lake Ice Concentration (LIC) products from Along-Track Scanning Radiometer (ATSR) imagery. Details of other sources of information associated with the generation and validation of these products are given in this section.

An outline of the selection process used to identify the target lakes for ARC-Lake is given in the ARC-Lake Technical Note on lake definition (MacCallum and Merchant, 2010).

The results of validation studies for the v1.2 LSWT and LIC products are given in the ARC-Lake Validation Report (MacCallum and Merchant 2011b).

The ARC-Lake v2.0 product file format is described in MacCallum and Merchant, (2011a). This document and the v2.0 data files are available for download from <http://hdl.handle.net/10283/88>. Additional information can be found on the ARC-Lake project website, <http://www.geos.ed.ac.uk/arclake>. Earlier v1.1 data files and associated documentation are available from <http://hdl.handle.net/10283/88>.

Further details of the Generalised Bayesian Cloud Screening (GBCS) methods on which are available from the GBCS website, <http://www.geos.ed.ac.uk/gbcs>. Bayesian cloud screening is also described in detail in Merchant *et al* (2005).


Useful information on the series of ATSR instruments is available from the following websites:

- <http://earth.esa.int/ers/atrs>
- <http://www.atsr.rl.ac.uk>

The radiative transfer model, RTTOV, is described in Brunel *et al* (2005). Additional information on RTTOV is available from: <http://research.metoffice.gov.uk/research/interproj/nwpsaf/rtm/>


The lake model, FLake, (Mironov, 2005) is available online at: <http://www.flake.igb-berlin.de/>

DINEOF, the software used to generate reconstructed temperature time series using principal component techniques, is described in Alvera-Azcárate (2005). Additional information is available from the DINEOF website: <http://modb.oce.ulg.ac.be/mediawiki/index.php/DINEOF>

<p>The University of Edinburgh</p> 	<p>ATSR Reprocessing for Climate Lake Surface Water Temperature – ARC-Lake</p>	<p>Document Ref: ARC-Lake-ATBD-v1.3 Issue: 1 Date: 23 Oct 2013</p>
--	--	--

12 References

- Alvera-Azcárate, A., Barth, A., Rixen, M., & Beckers, J. (2005). Reconstruction of incomplete oceanographic data sets using empirical orthogonal functions: application to the Adriatic Sea surface temperature. *Ocean Modelling*, 9(4), 325-346. doi: 10.1016/j.ocemod.2004.08.001.
- Beeton, A. M. (2002). Large freshwater lakes: present state, trends, and future. *Environmental Conservation*, 29(01), 21-38. doi: 10.1017/S0376892902000036.
- Brunel, P., English, S., Bauer, P., Keeffe, U. O., & Francis, P. (2005). RTTOV8 - Science and Validation Report, NWP SAF, EUMETSAT
- Cox, .C. and Munk, W. (1954), Measurement of the roughness of the sea surface from photographs of the Sun's glitter, *J. Opt., Soc., Am.*, 44, 838-850.
- Downing, H.D. and Williams, D. (1975), Optical constants of water in the infrared. *Journal of Geophysical Research*, 80, 1656–1661.
- ESRI: Environmental Systems Research Institute, (1993). Digital Chart of the World 1:1 Mio. Redlands, CA.
- Embury, O., Filipiak, M.J., & Merchant, C.J. (2010), A Reprocessing for Climate of Sea Surface Temperature from the Along-Track Scanning Radiometers: Basis in Radiative Transfer, submitted to *Remote Sensing of Environment*.
- Filiapiak, M. (2008). Refractive indices (500-3500 cm⁻¹) and emissivity (600-3350 cm⁻¹) of pure water and seawater, <http://hdl.handle.net/10283/17>
- GHR SST, (2006), <http://ghrsst.org/GHR SST-PP-NAVO-Land-and-sea-Mask.html>
- Herdendorf, C. E. (1982). Large Lakes of the World. *Journal of Great Lakes Research*, 8(3), 379-412. doi: 10.1016/S0380-1330(82)71982-3.
- Lehner, B., & Döll, P. (2004). Development and validation of a global database of lakes, reservoirs and wetlands. *Journal of Hydrology*, 296(1-4), 1-22. doi: 10.1016/j.jhydrol.2004.03.028.
- MacCallum, S. N. and C. J. Merchant (submitted 2011), Surface Water Temperature Observations of Large Lakes by Optimal Estimation, *Can J Remote Sensing*.
- MacCallum, S. N., and Merchant, C. J. (2011a), ARC-Lake Data Product Description – v1.1.2, School of GeoSciences, The University of Edinburgh, <http://hdl.handle.net/10283/88>.
- MacCallum, S. N., and Merchant, C. J. (2011b), ARC-Lake Validation Report – v1.2, School of GeoSciences, The University of Edinburgh.

<p>The University of Edinburgh</p> 	<p>ATSR Reprocessing for Climate Lake Surface Water Temperature – ARC-Lake</p>	<p>Document Ref: ARC-Lake-ATBD-v1.3 Issue: 1 Date: 23 Oct 2013</p>
---	---	--

MacCallum, S. N., and Merchant, C. J. (2011c), ARC-Lake v1.1, 1995-2009 [Dataset], The University of Edinburgh, School of GeoSciences / European Space Agency, <http://hdl.handle.net/10283/88>.

MacCallum, S. N., and Merchant, C. J. (2010), ARC-Lake Technical Note 1 - Lake Definition and Validation Strategy, School of GeoSciences, The University of Edinburgh.

Marmorino, G.O. and Smith, G.B. (2005), Bright and dark ocean whitecaps observed in the infrared. *Geophysical Research Letters*, 32, L11604, doi:10.1029/2005GL023176.

Marshall, J. H. (2003), Lake temperatures - thermal remote sensing and assimilation into a lake model, *PhD thesis*, The University of Edinburgh.

Masuda, K., Takashima, T. and Takayama, Y. (1988), Emissivity of pure and sea waters for the model sea surface in the infrared window region. *Remote Sensing of Environment*, 24, 313–329.

Masuda, K. (2006), Infrared sea surface emissivity including multiple reflection effect for isotropic Gaussian slope distribution model. *Remote Sensing of Environment*, 103, 488–496, .

Merchant, C. J., Harris, a. R., Maturi, E., & MacCallum, S. (2005). Probabilistic physically based cloud screening of satellite infrared imagery for operational sea surface temperature retrieval. *Quarterly Journal of the Royal Meteorological Society*, 131(611), 2735-2755. doi: 10.1256/qj.05.15.

Merchant, C., Leborgne, P., Marsouin, a., & Roquet, H. (2008). Optimal estimation of sea surface temperature from split-window observations. *Remote Sensing of Environment*, 112, 2469 - 2484. doi: 10.1016/j.rse.2007.11.011.


Mironov, D., Golosov, S., Heise, E., Kourzeneva, E., Ritter, B., Schneider, N., et al. (2005). FLake – A Lake Model for Environmental Applications. In *9th European Workshop on Physical Processes in Natural Waters* (pp. 2005-2005).

MODIS (2010), Ocean Level-3 Standard Mapped Image Products, http://oceancolor.gsfc.nasa.gov/DOCS/Ocean_Level-3_SMI_Products.pdf

Mutlow, C., Bailey, P., Birks, A., & Smith, D. (1999). ATSR-1 / 2 User Guide.

Newman, S.M., Smith, J.A., Glew, M.D., Rogers, S.M., and Taylor, J.P. (2005), Temperature and salinity dependence of sea surface emissivity, *Quarterly Journal of the Royal Meteorological Society*, 131, 2539-2557.

Oesch, D. C., Jaquet, J., Hauser, a., & Wunderle, S. (2005). Lake surface water temperature retrieval using advanced very high resolution radiometer and Moderate Resolution Imaging

<p>The University of Edinburgh</p> 	<p>ATSR Reprocessing for Climate Lake Surface Water Temperature – ARC-Lake</p>	<p>Document Ref: ARC-Lake-ATBD-v1.3 Issue: 1 Date: 23 Oct 2013</p>
---	---	--

Spectroradiometer data: Validation and feasibility study. *Journal of Geophysical Research*, 110(C12), 1-17. doi: 10.1029/2004JC002857.

Pinkley, L. W., & Williams, D. (1976). Optical properties of sea water in the infrared. *Journal of the Optical Society of America*, 66(6), 554. doi: 10.1364/JOSA.66.000554.

Pinkley, L.W., Sethna, P.P. and Williams, D. (1977), Optical constants of water in the infrared: Influence of temperature. *J. Opt. Soc. Am.*, 67, 494–499.

Reinhart, A., & Reinhold, M. (2008). Mapping surface temperature in large lakes with MODIS data. *Remote Sensing of Environment*, 112(2), 603-611. Elsevier. doi: 10.1016/j.rse.2007.05.015.

Rodgers, C. D. (1990). Characterization and Error Analysis of Profiles Retrieved From Remote Sounding Measurements. *Journal of Geophysical Research*, 95(D5), 5587-5595. doi: 10.1029/JD095iD05p05587.

Rodgers, C. D. (2000). *Inverse Methods for Atmospheric Sounding: Theory and Practice*. (F. W. Taylor). World Scientific.

Salisbury, J.W. and D'Aria, D.M. (1993), Thermal infrared remote sensing of crude oil slicks. *Remote Sensing of Environment*, 45, 225–231.


Stamnes, K., Tsay, S.C., Wiscombe, W., and Jayaweera, K. (1988), Numerically stable algorithm for discrete-ordinate-method radiative transfer in multiple scattering and emitting layered media, *Applied Optics*, 27 (12), 2502–2509.

Wan, Z. (2007). MODIS Land Surface Temperature Products Users' Guide, ICES, University of California, Santa Barbara

Wan, Z. (2008). New refinements and validation of the MODIS Land-Surface Temperature/Emissivity products. *Remote Sensing of Environment*, 112(1), 59-74. doi: 10.1016/j.rse.2006.06.026.

Watts, P.D., Allen, M.R., and Nightingale, T.J. (1996), Wind effects on the sea surface emission and reflection for the Along Track Scanning Radiometer, *J. Atmos. And Oceanic Technology*, 13, 126-141.


Wu, X.Q. and Smith, W.L.(1997), Emissivity of rough sea surface for 8-13 μm :modelling and verification, *Applied Optics*, 36, 2609-2619.

<p>The University of Edinburgh</p> 	<p>ATSR Reprocessing for Climate Lake Surface Water Temperature – ARC-Lake</p>	<p>Document Ref: ARC-Lake-ATBD-v1.3 Issue: 1 Date: 23 Oct 2013</p>
--	--	--


13 Appendix

13.1 Sources of data for prior LSWT field


ID	Name	Lon.	Lat.	ATSR-1				ATSR-2				AATSR			
				T	C	M	F	T	C	M	F	T	C	M	F
166	ABAYA	37.83	6.30			Y				Y				Y	
527	ABE	41.79	11.17	Y				Y				Y			
152	ABERDEEN	-98.59	64.55		Y					Y				Y	
418	ABY	-3.23	5.23		Y					Y		Y			
58	ALAKOL	81.75	46.11			Y		Y				Y			
30	ALBERT	30.91	1.67	Y				Y				Y			
210	ALEXANDRINA	139.09	-35.52	Y				Y				Y			
1748	ALMANOR	-121.19	40.26		Y			Y						Y	
56	AMADJUAK	-71.13	64.99		Y					Y				Y	
354	ANG-LA JEN	83.09	31.53		Y					Y		Y			
324	ANGIKUNI	-100.04	62.27		Y				Y				Y		
4	ARAL	60.08	45.13		Y				Y				Y		
117	ARGENTINO	-73.03	-50.33	Y				Y				Y			
334	ARTILLERY	-107.82	63.17		Y					Y				Y	
345	ASHUANIPI	-66.14	52.69		Y					Y				Y	
115	ASTRAY	-66.32	54.38		Y				Y				Y		
23	ATHABASCA	-109.96	59.10	Y				Y				Y			
311	ATLIN	-133.75	59.57		Y			Y						Y	
312	AYAKKUM	89.35	37.55	Y				Y				Y			
226	AYLMER	-108.46	64.15		Y					Y				Y	
181	BAGHRASH	87.07	41.98			Y		Y				Y			
8	BAIKAL	108.14	53.63	Y				Y				Y			
97	BAKER	-95.28	64.13		Y					Y				Y	
310	BALATON	17.83	46.88	Y				Y				Y			
17	BALKHASH	73.95	45.91	Y				Y				Y			
536	BANGONG	79.71	33.61		Y			Y				Y			
229	BARUN-TOREY	115.81	50.07	Y				Y				Y			
205	BAY	121.26	14.36	Y				Y				Y			
145	BECHAROF	-156.40	57.85	Y				Y				Y			
160	BELOYE	37.64	60.18	Y				Y				Y			
267	BEYSEHIR	31.52	37.78	Y				Y				Y			
155	BIENVILLE	-72.98	55.05		Y				Y					Y	
280	BIG TROUT	-90.02	53.77		Y			Y				Y			
268	BIWA	136.08	35.25			Y		Y				Y			
333	BLACK	-105.73	59.05		Y			Y				Y			
191	BRAS D'OR	-60.83	45.95			Y		Y				Y			
94	BUENOS AIRES	-72.50	-46.66	Y				Y				Y			
299	BUFFALO	-115.49	60.22			Y		Y				Y			
291	BUYR	117.69	47.81	Y				Y				Y			
257	CARATASCA	-83.85	15.35	Y				Y				Y			
1	CASPIAN	50.36	41.85	Y				Y				Y			
265	CAXUANA	-51.50	-2.04			Y		Y						Y	
57	CEDAR	-100.14	53.33	Y				Y				Y			
165	CHAMPLAIN	-73.27	44.45		Y					Y		Y			
233	CHAO	117.57	31.57	Y				Y				Y			
153	CHAPALA	-103.05	20.21	Y				Y				Y			
204	CHILKA	85.38	19.69	Y				Y				Y			

<p>The University of Edinburgh</p> 	<p>ATSR Reprocessing for Climate Lake Surface Water Temperature – ARC-Lake</p>	<p>Document Ref: ARC-Lake-ATBD-v1.3 Issue: 1 Date: 23 Oct 2013</p>
--	--	--


256	CHILWA	35.71	-15.32	Y				Y				Y			
84	CHIQUITA	-62.61	-30.74	Y				Y				Y			
119	CHISHI	29.72	-8.71	Y				Y				Y			
323	CHURCHILL	-108.29	55.96			Y		Y				Y			
125	CLAIRE	-112.08	58.59	Y				Y				Y			
1188	CLEAR	-122.77	39.02			Y		Y				Y			
275	CLINTON COLDEN	-107.45	63.94		Y			Y				Y			
277	COARI	-63.37	-4.25		Y			Y				Y			
219	COLHUE HUAPI	-68.76	-45.47	Y						Y		Y			
352	CONSTANCE	9.28	47.65			Y		Y				Y			
162	CONTWOYTO	-110.66	65.59		Y					Y				Y	
284	CORO	-69.86	11.56	Y				Y				Y			
137	CREE	-106.64	57.47		Y					Y		Y			
251	CROSS	-97.58	54.71		Y				Y				Y		
351	DAUPHIN	-99.77	51.27	Y				Y				Y			
244	DEAD	35.49	31.52	Y				Y				Y			
326	DESCHAMBAULT	-103.45	54.78			Y		Y				Y			
281	DORE	-107.28	54.76			Y		Y				Y			
49	DUBAWNT	-101.44	63.13		Y			Y				Y			
128	EAU CLAIRE	-74.40	56.15		Y			Y				Y			
297	EBI	82.92	44.86		Y			Y				Y			
305	EBRIE	-4.26	5.30		Y				Y				Y		
69	EDWARD	29.61	-0.39	Y				Y				Y			
390	EGRIDIR	30.85	38.07	Y				Y				Y			
254	ENNADAI	-101.31	60.96		Y					Y				Y	
723	ENRIQUILLO	-71.58	18.49	Y				Y				Y			
12	ERIE	-81.16	42.25	Y				Y				Y			
149	ESKIMO	-132.76	69.10		Y					Y				Y	
270	EVANS	-77.02	50.97		Y					Y				Y	
1029	EVORON	136.51	51.48		Y			Y						Y	
156	EYASI	35.04	-3.58		Y			Y					Y		
304	FAGNANO	-68.03	-54.55		Y			Y				Y			
315	FERGUSON	-105.27	69.41		Y			Y				Y			
404	FROBISHER	-108.22	56.37		Y					Y			Y		
227	GARRY	-99.40	65.95		Y					Y				Y	
327	GENEVA	6.25	46.37	Y				Y				Y			
172	GODS	-94.21	54.62		Y			Y				Y			
363	GRANVILLE	-100.21	56.40		Y				Y					Y	
252	GRAS	-110.38	64.54		Y					Y				Y	
9	GREAT BEAR	-121.30	65.91			Y				Y		Y			
11	GREAT SLAVE	-114.37	62.09			Y		Y				Y			
253	GUILLAUME-DELISLE	-76.28	56.33		Y					Y		Y			
294	HAR	93.21	48.05	Y				Y				Y			
142	HAR US	92.30	48.06	Y				Y				Y			
302	HAR-HU	97.59	38.31	Y				Y				Y			
214	HAUKIVESI	28.52	62.10		Y				Y					Y	
339	HAZEN	-70.94	81.80				Y				Y				Y
288	HIGHROCK	-100.44	55.83				Y				Y				Y
189	HOTTAH	-118.44	64.95		Y					Y				Y	
59	HOVSGOL	100.48	51.02			Y		Y						Y	
75	HULUN	117.38	48.97	Y				Y				Y			
109	HUNGTZE	118.53	33.34	Y				Y				Y			

<p>The University of Edinburgh</p> 	<p>ATSR Reprocessing for Climate Lake Surface Water Temperature – ARC-Lake</p>	<p>Document Ref: ARC-Lake-ATBD-v1.3 Issue: 1 Date: 23 Oct 2013</p>
--	--	--


5	HURON	-82.21	44.78	Y				Y				Y		
121	HYARGAS	93.30	49.13	Y				Y				Y		
62	ILIAMNA	-154.90	59.56	Y				Y				Y		
144	INARI	27.83	69.04		Y					Y			Y	
293	INDIAN RIVER	-80.64	28.24		Y					Y		Y		
174	ISLAND	-94.70	53.85		Y				Y				Y	
25	ISSYKKUL	77.25	42.46			Y		Y				Y		
1441	ISTADA	67.92	32.48			Y			Y				Y	
245	IZABAL	-89.11	15.57			Y		Y				Y		
141	KAGHASUK	-164.22	60.79		Y			Y				Y		
246	KAMINAK	-94.90	62.20		Y				Y				Y	
320	KAMINURIAK	-95.79	62.96		Y					Y			Y	
264	KAMILUKUAK	-101.73	62.28		Y					Y			Y	
287	KAoyu	119.31	32.87	Y				Y				Y		
197	KARA-BOGAZ-GOL	53.54	41.23	Y				Y				Y		
124	KASBA	-102.27	60.34		Y			Y				Y		
346	KEITELE	25.99	62.89		Y				Y				Y	
45	KHANKA	132.42	44.94	Y				Y				Y		
218	KHANTAYSKOE	91.18	68.36		Y					Y			Y	
67	KIVU	29.23	-2.04			Y		Y				Y		
41	KOKO	100.18	36.89	Y				Y				Y		
344	KRASNOE	174.44	64.53		Y			Y				Y		
262	KULUNDINSKOE	79.58	52.98	Y				Y				Y		
325	KWANIA	32.65	1.72		Y					Y		Y		
382	KYARING	88.32	31.13			Y		Y				Y		
99	KYOGA	33.01	1.50			Y		Y				Y		
331	LABAZ	99.57	72.27		Y			Y					Y	
16	LADOGA	31.39	60.84	Y				Y				Y		
147	LESSER SLAVE	-115.49	55.43	Y				Y				Y		
140	LIMFJORDEN	9.17	56.78	Y				Y				Y		
209	LLANQUIHUE	-72.79	-41.14	Y				Y				Y		
357	LOWER SEAL	-73.42	56.49				Y				Y			Y
175	LUANG	100.38	7.46		Y			Y				Y		
184	MACKAY	-111.30	63.96		Y					Y			Y	
101	MADRE	-97.66	24.64	Y				Y				Y		
163	MALAREN	16.19	59.44		Y					Y			Y	
350	MALHEUR	-118.83	43.34		Y					Y			Y	
176	MANAGUA	-86.35	12.32	Y				Y				Y		
231	MANGUEIRA	-52.84	-33.16	Y				Y				Y		
37	MANITOBA	-98.80	50.99	Y				Y				Y		
368	MANOUANE	-70.99	50.76		Y				Y				Y	
250	MANYCH-GUDILO	42.98	46.26	Y				Y				Y		
100	MARTRE	-117.91	63.33	Y				Y				Y		
6	MICHIGAN	-87.09	43.86	Y				Y				Y		
366	MILLE LACS	-93.65	46.24	Y				Y				Y		
224	MINTO	-74.71	57.34				Y				Y			Y
46	MIRIM	-53.25	-32.89	Y				Y				Y		
76	MISTASSINI	-73.81	50.82		Y					Y		Y		
883	MONO	-118.96	38.01			Y		Y					Y	
286	MURRAY	141.53	-6.95		Y				Y				Y	
36	MWERU	28.74	-9.01	Y				Y				Y		
343	NAHUEL HUAPI	-71.52	-40.92	Y				Y				Y		

<p>The University of Edinburgh</p> 	<p>ATSR Reprocessing for Climate Lake Surface Water Temperature – ARC-Lake</p>	<p>Document Ref: ARC-Lake-ATBD-v1.3 Issue: 1 Date: 23 Oct 2013</p>
--	--	--

377	NAKNEK	-155.67	58.64		Y				Y		Y		
91	NAM	90.66	30.71	Y				Y			Y		
322	NATRON	36.02	-2.34		Y				Y			Y	
338	NERPICH'YE	162.77	56.39		Y			Y			Y		
32	NETILLING	-70.28	66.42		Y				Y			Y	
300	NGORING	97.71	34.93	Y				Y			Y		
21	NICARAGUA	-85.36	11.57	Y				Y			Y		
38	NIPIGON	-88.55	49.80		Y			Y			Y		
198	NIPISSING	-79.92	46.24	Y				Y			Y		
211	NONACHO	-108.92	61.82		Y				Y				Y
303	NORTH MOOSE	-100.16	54.05			Y		Y			Y		
83	NUELTIN	-99.40	60.25		Y				Y				Y
10	NYASA	34.59	-11.96	Y				Y			Y		
114	OKEECIOBEE	-80.86	26.95	Y				Y			Y		
336	OLING	97.27	34.92	Y				Y			Y		
207	OMULAKH	145.59	72.29		Y				Y		Y		
18	ONEGA	35.35	61.90	Y				Y			Y		
15	ONTARIO	-77.77	43.85	Y				Y			Y		
187	ORIVESI	29.59	62.35		Y			Y					Y
157	PAIJANNE	25.49	61.71		Y				Y		Y		
697	PANGONG	78.61	33.82		Y				Y				Y
353	PAYNE	-73.82	59.40		Y				Y				Y
50	PEIPUS	27.59	58.41	Y				Y			Y		
349	PERLAS	-83.67	12.54			Y		Y			Y		
222	PETER POND	-108.55	55.84			Y		Y			Y		
195	PIELINEN	29.71	63.16		Y				Y				Y
213	PLAYGREEN	-97.75	54.07		Y			Y			Y		
232	POINT	-113.84	65.31		Y				Y			Y	
649	POMO	90.40	28.55		Y				Y				Y
133	POOPO	-67.06	-18.81		Y				Y		Y		
395	PRINCESS MARY	-97.66	63.93		Y				Y				Y
164	PURUVESI	29.02	61.77		Y				Y				Y
273	PYA	30.98	66.07		Y				Y				Y
240	PYASINO	87.78	69.77		Y			Y			Y		
1240	PYHAJARVI	22.28	61.00		Y			Y			Y		
411	PYRAMID	-119.55	40.03	Y				Y			Y		
130	RAINY	-92.97	48.61		Y				Y				Y
358	RAZELM	28.97	44.83	Y				Y			Y		
151	RED	-95.08	48.04	Y				Y			Y		
28	REINDEER	-102.27	57.19		Y			Y			Y		
321	ROGOAGUADO	-65.73	-12.91		Y				Y		Y		
127	RONGE	-104.83	55.11		Y			Y			Y		
22	RUDOLF	36.08	3.53	Y				Y			Y		
146	SAINT CLAIR	-82.73	42.50	Y				Y			Y		
158	SAINT JEAN	-72.02	48.66			Y		Y			Y		
285	SAINT JOSEPH	-90.81	51.04		Y				Y				Y
282	SAKAMI	-76.75	53.22		Y				Y				Y
194	SALTON	-115.83	33.30	Y				Y			Y		
167	SAN MARTIN	-72.84	-48.75		Y			Y			Y		
356	SANDY	-93.03	53.00		Y				Y				Y
241	SARYKAMYSHSK OYE	57.61	41.88	Y				Y			Y		
247	SASYKKOL	80.91	46.58			Y		Y			Y		

<p>The University of Edinburgh</p> 	<p>ATSR Reprocessing for Climate Lake Surface Water Temperature – ARC-Lake</p>	<p>Document Ref: ARC-Lake-ATBD-v1.3 Issue: 1 Date: 23 Oct 2013</p>
--	--	--

313	SCOTT	-106.07	60.02		Y				Y				Y		
228	SEG	33.76	63.32		Y			Y				Y			
170	SELAWIK	-160.73	66.51			Y				Y		Y			
271	SELETYTENIZ	73.18	53.23			Y				Y		Y			
292	SELWYN	-104.68	60.00		Y				Y					Y	
135	SEVAN	45.29	40.39	Y				Y				Y			
579	SHAMO	37.55	5.83			Y				Y				Y	
143	SHERMAN	-97.73	67.79		Y					Y				Y	
236	SIMCOE	-79.42	44.47	Y				Y				Y			
27	SMALLWOOD	-64.31	54.19		Y			Y				Y			
365	SNOWBIRD	-102.94	60.64		Y			Y				Y			
319	SOUTH HENIK	-97.29	61.37		Y					Y				Y	
225	SOUTH MOOSE	-100.04	53.83			Y		Y				Y			
2	SUPERIOR	-88.23	47.72	Y				Y				Y			
85	SYVASH	34.74	45.96			Y		Y				Y			
380	TAHOE	-120.04	39.09	Y				Y				Y			
66	TAI	120.24	31.21	Y				Y				Y			
178	TAKIYUAK	-113.17	66.28		Y					Y				Y	
235	TAMIAHUA	-97.57	21.66	Y				Y				Y			
55	TANA	37.31	11.95	Y				Y				Y			
7	TANGANYIKA	29.46	-6.07	Y				Y				Y			
215	TANGRA	86.59	31.05	Y				Y				Y			
73	TAPAJOS	-55.14	-2.88	Y				Y				Y			
316	TATHLINA	-117.64	60.54	Y				Y				Y			
295	TAUPO	175.90	-38.81	Y				Y				Y			
43	TAYMYR	100.76	74.48		Y				Y				Y		
373	TEBESJUAK	-98.98	63.76		Y					Y				Y	
120	TENGIZ	68.90	50.44	Y				Y				Y			
179	TERINAM	85.61	30.90	Y				Y				Y			
212	TESHEKPUK	-153.60	70.59		Y			Y				Y			
20	TITICACA	-69.30	-15.92	Y				Y				Y			
150	TOBA	98.90	2.61		Y					Y				Y	
186	TOP	32.09	65.62		Y					Y				Y	
332	TOWUTI	121.52	-2.79			Y				Y				Y	
367	TROUT	-121.13	60.58	Y				Y				Y			
269	TULEMALU	-99.48	62.99		Y			Y						Y	
255	TUMBA	17.98	-0.82		Y					Y		Y			
425	UBINSKOE	80.05	55.47	Y				Y				Y			
239	ULUNGUR	87.30	47.22	Y				Y				Y			
314	UPEMBA	26.40	-8.65	Y				Y				Y			
53	UVS	92.81	50.33	Y				Y				Y			
51	VAN	42.98	38.66	Y				Y				Y			
29	VANERN	13.22	58.88	Y				Y				Y			
95	VATTERN	14.57	58.33	Y				Y				Y			
1820	VESIJARVI	25.39	61.09		Y				Y					Y	
3	VICTORIA	33.23	-1.30	Y				Y				Y			
171	VIDMA	-72.56	-49.59	Y				Y				Y			
136	VYG	34.84	63.54		Y			Y				Y			
1128	WALKER	-118.71	38.70			Y		Y				Y			
876	WEISHAN	117.24	34.61	Y				Y				Y			
169	WHOLDAIA	-104.15	60.69		Y				Y				Y		
340	WINNEBAGO	-88.42	44.02	Y				Y				Y			
13	WINNIPEG	-97.25	52.12	Y				Y				Y			

<p>The University of Edinburgh</p> 	<p>ATSR Reprocessing for Climate Lake Surface Water Temperature – ARC-Lake</p>	<p>Document Ref: ARC-Lake-ATBD-v1.3 Issue: 1 Date: 23 Oct 2013</p>
---	---	--

31	WINNIPEGOSIS	-100.05	52.37	Y				Y				Y			
68	WOLLASTON	-103.33	58.30		Y			Y				Y			
44	WOODS	-94.91	49.38	Y				Y				Y			
134	XINGU	-52.20	-2.16	Y				Y				Y			
261	YAMDROK	90.76	28.97		Y				Y				Y		
126	YATHKYED	-98.07	62.69		Y					Y		Y			
105	ZILING	88.95	31.77	Y				Y				Y			

Table 5. Breakdown of sources of data for the prior LSWT field (§4)